Received: 27 February 2023 | Revised: 28 June 2023 | Accepted: 12 July 2023

DOI: 10.1111/bre.12809

Basin Research | IAS EAGE | WILEY

RESEARCH ARTICLE

Syn- and post-rift lower crustal flow under the Sunda Shelf, southern Vietnam: A role for climatically modulated erosion

Peter D. Clift[1,2] | **Leora J. Wilson**[2]

[1]Department of Earth Sciences, University College London, London, UK

[2]Department of Geology and Geophysics, Louisiana State University, Baton Rouge, Louisiana, USA

Correspondence
Peter D. Clift, Department of Earth Sciences, University College London, 5 Gower Place, London WC1E 6BS, UK.
Email: peter.clift@ucl.ac.uk

Funding information
Charles T. McCord Jr Chair in Petroleum Geology

Abstract

Tectonic subsidence on rifted, passive continental margins are largely controlled by patterns of extension and the nature of strain partitioning in the lithosphere. The Sunda Shelf, adjacent to the SW South China Sea, is characterized by deep basins linked to regional Cenozoic extension associated with propagating seafloor spreading caused by slab pull from the south. Analysis of seismic reflection profiles and drilled sections crossing the Nam Con Son and Cuu Long basins highlight Oligocene extension, with most of the thinning concentrated in the ductile mid-lower crust. Upper crustal extension was modest and ductile flow is inferred to be directed northwestwards, towards the oceanic crust. Basin inversion occurred in the Mid Miocene, associated with the collision of the Dangerous Grounds Block and Borneo. Subsequent accelerated tectonic subsidence exceeded predictions from uniform extension models assumed to relate to extensional collapse after inversion. We correlate this to a period of faster erosion onshore driven by strong monsoon rains in Indochina and Peninsular Thailand at that time. Erosion of the onshore basement, inducing rock uplift and coupled with loading of the basins offshore, drives ductile mid-lower crustal flow, likely to the northeast under Indochina, and/or to the west where Plio-Pleistocene subsidence of the shelf is very slow. Significant sediment delivery from the Mekong River into the Cuu Long Basin began in the Late Miocene and migrated seawards as the basin filled. Mass balancing suggests that the basins of this part of the Sunda Shelf are filled through erosion of bedrock sources around the Gulf of Thailand. There is no need for sediment delivery from a major river draining the Tibetan Plateau to account for the deposited volumes.

KEYWORDS

inversion, Mekong River, sediment budget, South China Sea, Subsidence

1 | INTRODUCTION

Lithospheric extension during the break-up of continents and the subsequent opening of ocean basins results in significant tectonic subsidence, mostly caused by isostatic effects related to the thinning of the pre-existing continental crust (Bott, 1992; McKenzie, 1978; Royden & Keen, 1980). However, the degree of subsidence observed on many continental margins greatly exceeds that which might be expected from the degree of brittle extensional faulting in the upper crust, as imaged in seismic reflection profiles (Driscoll & Karner, 1998; Lister et al., 1991). Explanations for this excess subsidence have been strongly contested within the basin analysis community. Some argue for a dominant role for low-angle detachment faulting. In these models, excess lower crustal extension is inferred to account for the anomaly and is considered to be removed and preserved under the opposing conjugate passive margin (Froitzheim & Rubatto, 1998; Lister et al., 1986; Reston et al., 1996). Alternatively, others have proposed ductile lower crustal flow towards the oceanic crust under both conjugate margins. This results in higher thinning of the lower crust, and thus greater total extension than inferred from the faulting alone (Clift et al., 2002; Davis & Kusznir, 2004; Hopper & Buck, 1996).

Uniform pure shear models for the deformation of the continental lithosphere suggest that areas where there is significant upper crustal faulting should experience substantial amounts of subsidence after, as well as during, active extension (McKenzie, 1978). This is because the lower crust and mantle lithosphere should also be extended to the same degree as the upper crust, although not necessarily in the same location. The thinned mantle lithosphere then cools and thickens after active extension, causing thermal subsidence due to isostatic effects. While this is often true in intracontinental rift systems, this rule breaks down on passive margins. Areas with weak lithosphere are often associated with thick, warm and ductile crust, such as in magmatic arcs or orogenic belts (Buck, 1991; Maggi et al., 2000). These regions are prone to non-uniform extension as a result of the flow of the ductile crust below the level of normal faulting (ca. 10–15 km) (Brune et al., 2017). This model has been applied to many of the basins surrounding the South China Sea (Clift et al., 2002; Davis & Kusznir, 2004; Huang et al., 2021; Sun et al., 2009), which was an area of active margin magmatism during the Jurassic-Cretaceous (Jahn et al., 1990; Li, Zhang, et al., 2014). This preceded the onset of extension that peaked in the Oligocene, at least in the central and eastern parts of the basin (Li, Xu et al., 2014; Su et al., 1989).

Although numerous studies of the northern margin of the South China Sea have examined the strain accommodation during continental break-up, a similar analysis of the conjugate southern side has been more difficult as a result of poor access and sparse data (Clift et al., 2002; Franke et al., 2011). Furthermore, the collision of this southern margin with Borneo along its southern edge has complicated the vertical tectonics because of flexure of the Dangerous Grounds margin into the trench, inducing additional tectonically triggered vertical motions (Clift, Lee, et al., 2008; Franke et al., 2008; Hutchison, 2010).

If we wish to quantify the competing influences of syn-rift and post-rift tectonic processes on the vertical motion of conjugate margins, it is important to understand how the margin behaved before the onset of seafloor spreading. This can be difficult because the syn-rift strata are mostly continental, poorly dated and often not deeply drilled offshore southern China. In this study, we examine the Sunda Shelf of Southeast Asia, which is located immediately in front of the now-dead propagating seafloor spreading centre of the South China Sea (Figure 1) (Lee et al., 2001; Li, Clift, et al., 2014; Matthews et al., 1997). This area should represent only the effects of extension prior to seafloor spreading, which never reached this far to the southwest and allows us to understand the role played by crustal flow prior to continental break-up. We attempt to quantify the degree of upper and lower crustal extension in order to estimate how the strain was partitioned during the final stages of continental break-up. We also seek to date the timing of lower crustal flow relative to the rift tectonics and to see if any flow postdates active rifting (Clift et al., 2015). We correlate the subsidence history with well-known regional tectonic and climatic events, as well as the sediment loading in this area, in order to test their influence on basin formation, especially in the form of lower crust flow.

We use seismic profiles collected originally for oil and gas exploration, together with age constraints derived from four drilling sites along the eastern edge of the shelf,

Highlights

- Subsidence of the eastern Sunda Shelf exceeds what is predicted from upper crustal faulting.
- Ductile flow of the mid-lower crust towards the oceanic crust occurred during breakup.
- Sediment loading after 10 Ma caused ductile flow of the mid-lower crust towards Indochina and to the west.
- Increased sediment flux is partly driven by a stronger summer monsoon in the Pliocene.
- The sediment volumes in the basins are explicable by erosion around the Gulf of Thailand with no need for input from a large Tibetan river.

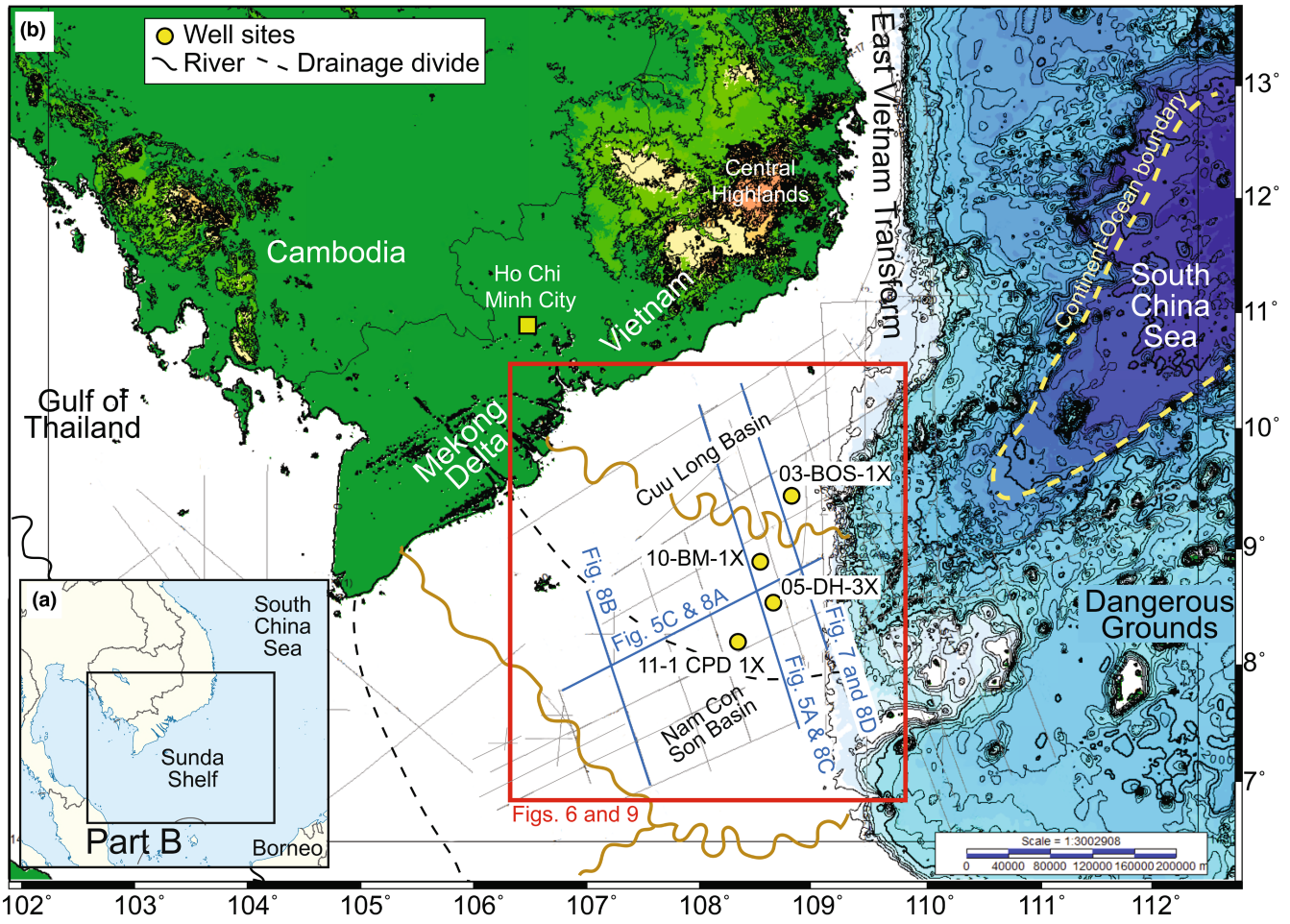

FIGURE 1 Topographic and bathymetric map of the study area south of the Mekong Delta. Black lines show the location of the seismic profiles which form the basis of this work. Wavy brown lines indicate the approximate position of paleo-river systems that would have occupied the shelf during sea-level low stands, with dashed black lines separating these. The continent–ocean boundary is from Huchon et al. (2001).

which allow the stratigraphy to be assigned to specific age intervals. Together these data allow us to constrain the sedimentation history of the shelf and to quantify the vertical tectonics since the Early Miocene (<24 Ma), allowing the degrees of extension across the region to be resolved. In doing so we are able to quantify the strain accommodation within the lithosphere and test for linkages between onshore erosion driven by climatic or tectonic processes and subsidence offshore.

1.1 | Geological setting

We focus on two major sedimentary basins that lie south of the Indochina peninsula in the south-western South China Sea. The basins underlie the modern Sunda Shelf and are known as the Cuu Long and Nam Con Son basins (Figure 1). They represent the product of regional Cenozoic extension, largely related to the southwestward propagation of continental rifting and seafloor spreading in the South China Sea (Lee et al., 2001; Matthews et al., 1997; Schmidt et al., 2019). This initiated further towards the northeast during the Early Eocene (Lei et al., 2019) and propagated to the southwest until 17 Ma when seafloor spreading stopped (Li, Li, et al., 2015). Seafloor spreading ceased immediately in front of the modern Sunda Shelf edge, as shown by the identification of a continent–ocean boundary (COB) offshore southeast Vietnam (Huchon et al., 1998, 2001) (Figure 1). The regional extension is complicated by transform tectonics along the East Vietnam margin, representing a southward extension of strike-slip motion along the Red River Fault Zone (RRFZ) (Fyhn et al., 2009; Roques et al., 1997; Vu et al., 2017). Further west, there is additional transform and pull-apart extension in the Gulf of Thailand where major transtensional basins have developed, most notably the Pattani Trough, and the Penyu, Malay and West Natuna basins (Fyhn et al., 2010; Madon & Watts, 1998; Schmidt et al., 2019; Tjia & Liew, 1996) (Figure 2). Together these basins underlie the largest tropical shelf region on Earth.

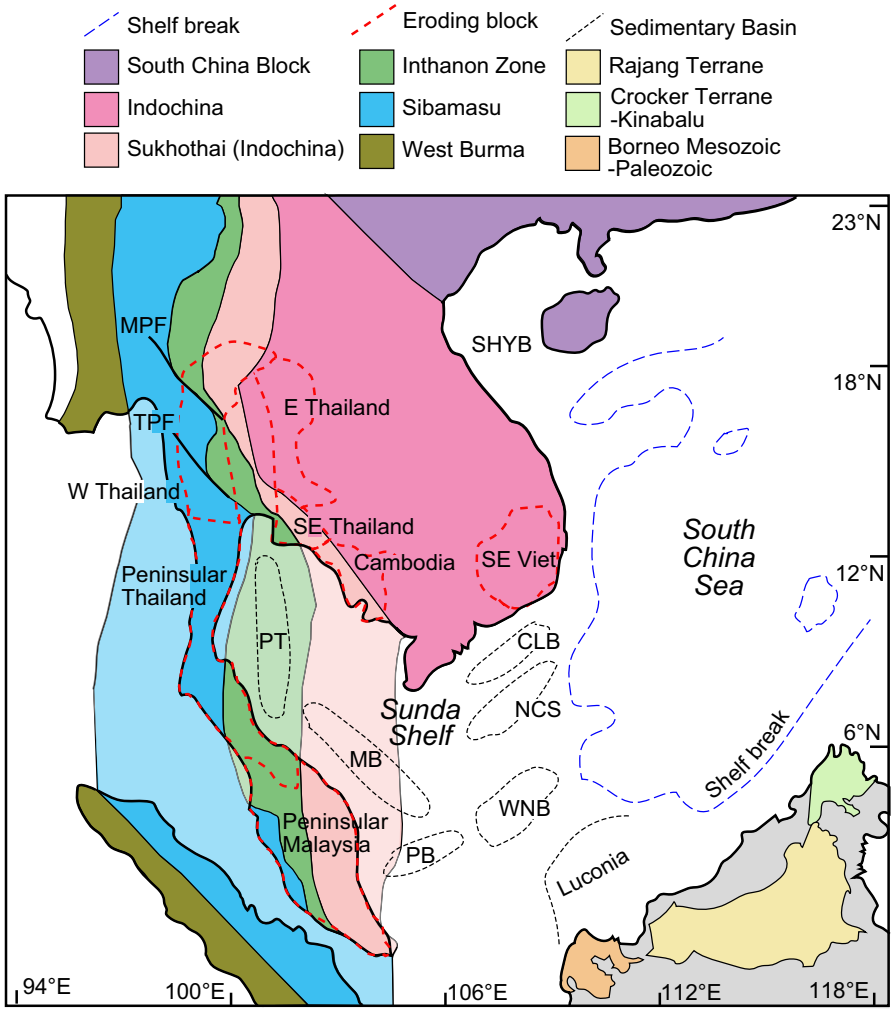

FIGURE 2 The tectonic terrane map of SE Asia and Borneo shows the major blocks whose erosion may fill the sedimentary basins of the Gulf of Thailand and Sunda Shelf. Blocks of SE Asia and Sumatra are from Morley and Searle (2017) and in Borneo from Hutchison (2005). CLB, Cuu Long Basin; MB, Malay Basin; MPF, Mae Ping Fault Zone; NCS, Nam Con Son Basin; PB, Penyu Basin; PT, Pattani Trough; SHYB, Song Hong-Yinggehai; TPF, Three Pagoda Fault Zone; WNB, West Natuna Basin.

Debate continues concerning the origin of the South China Sea, but a common view is that the extension terminated after the southern margin of this basin (i.e., the Dangerous Grounds continental block) collided with Borneo. In this model, extension in the modern South China Sea was driven by the subduction of a Paleo-South China Sea towards the southeast under Borneo (Clift, Lee, et al., 2008; Hall, 1996; Hinz et al., 1989; Hutchison, 2010; Hutchison et al., 2000). As the southern margin, now preserved as the Dangerous Grounds Block collided with and underthrust Borneo, the slab-pull effect from the Paleo-South China Sea lithosphere would have ceased and seafloor spreading discontinued. This collision is often believed to have generated the widespread Middle Miocene 'Deep Regional Unconformity' (DRU) across the southern South China Sea (Hutchison, 2005; Morley, 2016). The unconformity represents the product of erosion following basin inversion, which is a characteristic of the Sunda Shelf, as well as parts of northern Borneo (Hutchison, 2005). The age of the DRU has been debated with an age of 12–13 Ma proposed by Lunt (2019), postdating the earlier onset of collision in the Dangerous Grounds prior to 16 Ma (Morley et al., 2022).

The extended crust under the Sunda Shelf forms part of the larger Sundaland continental block, which has sometimes been considered a relatively strong and rigid piece of the lithosphere (Peltzer & Tapponnier, 1988). This together with Indochina was extruded via strike-slip faults towards the southeast as a result of continental collision in the area of the Tibetan Plateau (Replumaz & Tapponnier, 2003; Tapponnier et al., 1982). However, whether Sundaland can really be considered as being structurally rigid is debated because of the Neogene bending of Borneo relative to the rest of Sundaland (Hall, 2002), paleomagnetic evidence for deformation within Indochina (Cung & Geissman, 2013), and the presence of basins such as those we consider here that require deformation within Sundaland (Hall & Morley, 2004; Lee & Lawver, 1995; Pubellier & Morley, 2013). The general recognition that extension in the South China Sea is in a 'wide rift' mode, like the Basin and Range, based on the wide continent–ocean transition and high heat flow, argues for the lithosphere being weak and deformable (Burton-Johnson & Cullen, 2022; Clift et al., 2001).

Since the end of seafloor spreading, this region was disturbed by the emplacement of the Miocene flood basalt province in the Central Highlands of Vietnam (Hoang

& Flower, 1998; Hoang et al., 1996). Eruptions mostly spanned from 16 to 5 Ma and were associated with regional uplift and exhumation that reached a peak after around 8 Ma (Carter et al., 2000). It is not yet apparent what caused this volcanism since the region does not appear to be underlain by a mantle plume, at least one of a strong Hawaiian or Icelandic character, although it has been suggested that tectonic extrusion drove asthenospheric upwelling and caused the partial removal and replacement of the lithospheric mantle (Hobbs, 2020). There is some evidence for geochemical anomalies in the source mantle that have resulted in correlation to the "Hainan Plume" (An et al., 2017), but little suggestion of the regional uplift that is usually related to the presence of a major mantle thermal anomaly (Sleep, 1990). Regional subsidence studies have shown that depth anomalies are modest and that any temperature difference with ambient upper mantle is small (Wheeler & White, 2000). Indeed, some geodynamic models represent this region as overlying a number of subducted slabs and would instead represent a cold area in the upper mantle (Lithgow Bertelloni & Gurnis, 1997).

The Sunda Shelf is noted for its shallow water depths and flat bathymetry because the underlying sedimentary basins are largely full of sediment supplied from the surrounding continents. In more recent geologic times, this sediment has been dominated by supply from the Mekong River that drains Indochina and the southeast flank of the Tibetan Plateau (Clift et al., 2006; Jagodziński et al., 2020). The age of initiation of the Mekong is debated, although earlier analysis of large clinoforms along the shelf edge suggested that the Mekong only started to deposit in this area during the latter part of the Late Miocene (Li et al., 2013; Murray & Dorobek, 2004). Changes in the composition of the sediment offshore imply that the earliest initiation of the Mekong Delta in this region was around 8 Ma (Liu et al., 2017).

2 | METHODS

2.1 | Seismic stratigraphy

We employ standard seismic stratigraphic methods to divide the sedimentary fills of these basins into depositional units separated by sequence boundaries that are typically disconformities or unconformities (Vail et al., 1977; Van Wagoner et al., 1988). We also trace dated horizons from the drilling sites across the continental shelf, following continuous reflections as far as possible. Drilling depths were converted to two-way travel time (TWT) using the stacking velocities generated during the seismic processing. The interpretation of the seismic data was done using *IHS Kingdom*™ software. The interpretations were subsequently exported in order to use them for two-dimensional subsidence analysis. A time–depth conversion was made using an average interval velocity derived from the stacking velocities in a central part of the Cuu Long Basin, considered to be a typical example. We used an average of the velocity structure at three successive shot point locations for which data were available to eliminate any local anomalies. The velocity model is provided in Table 1 and shown graphically in Figure 3. Using this velocity versus depth at this point, we were able to determine the average interval velocity for each of the stratigraphic packages interpreted in this study at the same location. This velocity was then applied to the TWT for the bottom of each package in turn in order to calculate its depth across the basin. There was no attempt to account for lateral variations within a single package. This conversion represents one of the largest uncertainties in our analysis because there is lateral variability in subsurface velocities within a single depositional package linked to lithological heterogeneity and different degrees of compaction that may result in uncertainties on the order of ±20% (Clift, 2006). In the absence of suitable refraction seismic data and lack of access to sonic well logs, this is a reasonable approximation.

2.2 | One-dimensional subsidence analysis

One-dimensional backstripping analysis was performed on the sections sampled at the industrial wells using the method of Sclater and Christie (1980). This involves progressive unloading of the basement and correction for both sediment and water loading caused by variations in global sea level (Miller et al., 2020) as well as burial compaction. This progressive removal of each dated sedimentary unit is known as backstripping and was done in order to isolate the tectonic components of the subsidence. This analysis assumes local isostatic equilibrium, which may be justifiable if the flexural rigidity of the lithosphere is low. In general, sedimentary basins with extension >30% are considered to have a flexural rigidity of only ca. 5 km during active extension, making this a reasonable approximation (White, 1999). Furthermore, analysis of the continental margins around the South China Sea shows that modern-day flexural rigidity is still low, typically ca. 8 km under the Dangerous Grounds and the South China Shelf (Braitenberg et al., 2006; Clift et al., 2002; Lin & Watts, 2002; Xie et al., 2017). We use two-dimensional basin modelling methods to test this approximation. Even if the magnitudes of subsidence reconstructed by the one-dimensional approach are not entirely accurate, they provide the opportunity to identify periods of accelerated subsidence that are often associated with active extension. They also provide a general assessment of the total amount of subsidence, and

TABLE 1 Upper panel: velocity model used for the conversion of interpreted time sections to depths for backstripping. Lower panel: velocity data from Line SCSC-20 was used to construct the velocity-depth model.

Stratigraphic unit	Interval velocity (m/s)
Seawater	1500
Uppermost Pleistocene	1600
Upper Pleistocene	1620
Mid-Pleistocene	1630
Lower Pleistocene	1640
Upper Pliocene	1645
Lower Pliocene	1650
Upper Miocene	1670
Middle Miocene	1850
Lower Miocene	2300
Oligocene	2750

TWT (s)	VRMS (m/s)	Depth (m)	Depth (mbsf)	Interval thickness (m)	Interval velocity (ms)
0.089	1480	66			
0.497	1709	425	359	359	1759
0.943	1998	942	876	517	2320
1.289	2203	1420	1354	478	2762
1.649	2407	1985	1919	565	3137
1.996	2602	2597	2531	612	3529
2.459	2812	3457	3391	861	3717
3.000	3041	4562	4496	1104	4082
3.573	3229	5769	5703	1207	4213
4.064	3372	6852	6786	1083	4413
5.000	3547	8868	8802	2016	4307

Abbreviations: mbsf, meters below seafloor; TWT, two-way travel time; VRMS, root mean squared velocity.

therefore of total crustal extension independent of the two-dimensional analysis (McKenzie, 1978).

Because none of the drilling sites penetrated as far as the pre-rift basement at any location, we examine a synthesized complete section to allow a more comprehensive analysis. We look at the total amount of extension using a combination of the drilling data from the shallower levels and a seismically derived estimate of the thickness of older, deeper sediment at well 11-1 CPD 1X (Figure 1). This synthetic 'pseudo-well' represents an image of the complete section in the Nam Con Son Basin and allows us to derive an overall image of the total amount of subsidence, at least along the eastern margin of the shelf.

2.3 | Two-dimensional subsidence analysis

We selected a number of the better-quality seismic profiles to undertake two-dimensional subsidence analysis. The interpretations exported from *IHS Kingdom* were loaded into the *FlexDecomp*™ program of Badley Geoscience Ltd. This program was then used to sequentially remove the interpreted sedimentary layers in order to estimate the total modern depth to the basement after correcting for the sediment loading. The backstripping involved no correction for thermal subsidence so the final result is a prediction of the depth the basement would be at in the present day if there had been no sedimentation. We use an effective elastic thickness (Te) of 8 km as a reasonable estimate of the modern rigidity, as this yielded consistent results in earlier studies (Davis & Kusznir, 2004).

The unloaded modern depth to the basement can then be used to estimate the total amount of crustal extension along the profile, assuming negligible flexural rigidity and the uniform pure shear extensional model of McKenzie (1978) to estimate thermal subsidence. In this model, we assume a pre-rift crustal thickness of 30 km and a lithospheric thickness of 125 km because this predicts the top of the crust to be near sea level at the start of

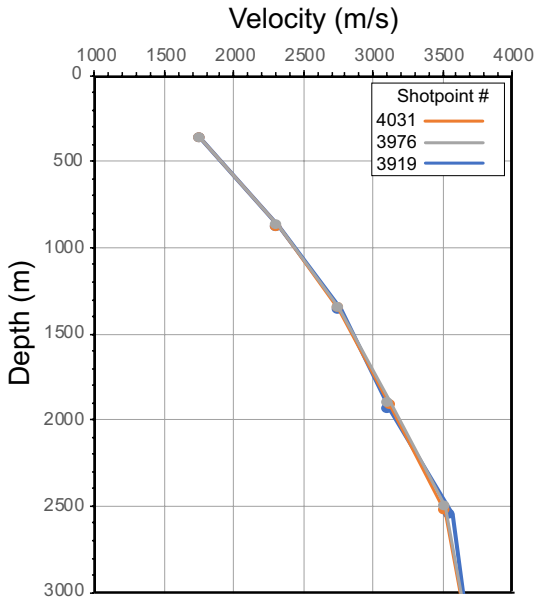

FIGURE 3 Seismic velocity versus depth at the intersection of profiles SCSC-05 and SCSC-20 (8.42038692° N, 108.0578539° E), which was used as a typical example for time-depth conversion (see Table 1).

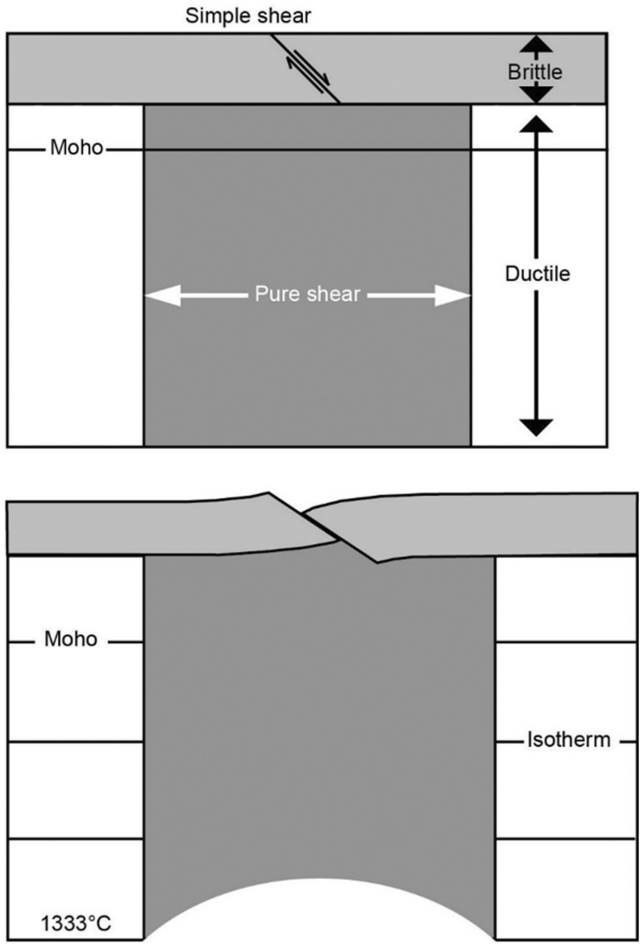

FIGURE 4 A schematic representation of the flexural cantilever model for lithospheric deformation, showing assumptions of simple shear faulting in the brittle upper crust and the assumed same amount of pure shear in the lower crust and mantle (redrawn from Kusznir et al., 1991).

extension and these values provide relatively good agreement with one-dimensional backstripping of drilled sections in the northern South China Sea (Clift et al., 2002). Moreover, 30 km is close to the estimate of the relatively unextended crust close to the coast measured by refraction profiles (Nissen et al., 1995; Zhang et al., 2018). In order to make this estimate, we have to decide on the age of the end of extension. Although the age of inversion and the end of the associated significant brittle faulting is ca. 16 Ma (Lee et al., 2001; Matthews et al., 1997; Morley et al., 2011), we choose to use 24 Ma for this purpose because it results in more consistent estimates of extension and represents the time that the strongest extension under the Sunda Shelf finished.

By quantifying the total modern sediment-unloaded depth to the basement along a profile, the total crustal extension can be estimated based on the uniform extension model (McKenzie, 1978). These values can be compared with the total upper crustal extension that is measured from the horizontal extension measured across normal faults in the seismic profiles. Because of the long wavelengths used in deep-penetrating seismic reflection imaging in oil and gas exploration, smaller faults are necessarily missed, accounting for as much as 40% of the total upper crustal extension (Walsh et al., 1991). Because of the general orientation of the basins and the magnetic fabrics in the oceanic South China Sea, we anticipate that extension was largely oriented NW-SE. Consequently, we choose to focus on seismic profiles that are oriented in this direction, while connected by a series of crossing lines in the perpendicular direction. This was done to provide some coverage across most of the basin, in order to map out the patterns of extension. The measured offsets and throw directions for each fault were measured and entered into the *Stretch*™ program of Badley Geoscience Ltd. This program models basin formation based on throws on normal faults and applied to the flexural cantilever extension model, where ductile deformation is distributed over 100 km wavelengths (Kusznir et al., 1991) (Figure 4). In this case, we primarily use this for estimating the lateral variability in upper crustal extension.

If the degrees of upper and total crust extension are known, then the lower crustal extension can be estimated, assuming a depth of the brittle-to-ductile transition. The depth of this transition depends on the composition of the continental crust, as well as the heat flow, although in general it is estimated to lie between 10 and 15 km in depth for felsic lithologies (Doglioni et al., 2011; Rutter, 1986). The

brittle-to-ductile transition shallows during extension as heat flow increases (Lavier & Manatschal, 2006), while becoming deeper later as the lithosphere cools or its extension becomes very high (Pérez-Gussinyé et al., 2006). Previous estimates of extension in the Nam Con Son Basin indicate up to a β factor of ca. 1.5 that implies a geothermal gradient of ca. 44°C/km at the end of active extension (McKenzie, 1978) and therefore a depth of 6.8 km to the 300°C isotherm, the temperature at which quartz is ductile (Scholz, 1998). However, deep-penetrating seismic profiles of the Nam Con Son Basin show faults ending in the mid-crust ca. 7 s TWT (Franke et al., 2014), suggesting >15 km depths. Because the South China Sea represents the product of rifting shortly after the cessation of active continental margin magmatism, it might be expected that the brittle–ductile transition would be shallow because of the high heat flow in a tectonically active setting (Jahn et al., 1990). Consequently, we use the value of 10 km as an estimate for the base of the brittle deforming zone in the upper crust (Clift et al., 2002). Because the lithospheric strength in such settings is focused on the brittle upper crust, a relatively thin estimate of the upper crust is consistent with our understanding of a relatively low flexural rigidity (Maggi et al., 2000).

2.4 | Sediment budgets

We reconstruct the sedimentation budget of the basins by performing a two-dimensional backstripping analysis on a select number of the interpreted and depth-converted profiles. This process involves the progressive removal of each dated sedimentary layer and then correction for the compaction that would have occurred as a result of burial under the younger layers. The decompaction procedure follows the methods of Sclater and Christie (1980) and since we do not know the lithologies to the base of the section and cannot account for lateral variability we use an intermediate silt average lithology to perform the decompaction. We use the same compaction correction method applied in the one- and two-dimensional backstripping. We use the duration of each depositional package taken from the biostratigraphy and converted to numerical ages using the Gradstein et al. (2020) timescale. These ages are used to calculate the rate of sedimentation in square kilometres per million years for each line. Three lines (SCSC-9, -20 and -22) are oriented across the strike of the basins and two (SCSC-09 and SCSC-21) lie along the axis of the Nam Con Son Basin in order to account for variations in sediment accumulation in both directions. The analysis of two-dimensional sections is more representative than single boreholes because it allows us to account for sediment wherever it is preserved within the shelf system, thus accounting for variable tectonically controlled accommodation space.

Interpretations show a clear thickening of sediment towards the continental margin and our analysis accounts for this variability. In order to derive a basin-wide estimate, the sedimentation rates for each of the lines were added together to provide a combined total budget. This was then normalized and applied to the total estimated sedimentary volume of the basin. By taking this approach, we give greater weight to the longest lines, but this is appropriate because they span a greater area and should be more representative of the regional average than short lines. In doing this, we follow the earlier approach of Clift et al. (2006). The volumetric estimates reflect the decompacted volumes so that each successive package of material can be realistically compared. The volume may then be converted into a deposited weight of eroded rock by accounting for the 50% porosity present in newly deposited silty sediment (Sclater & Christie, 1980). Silt may be considered a good average and comprises much of the sedimentary mass in many marine sedimentary basins, being intermediate between coarser sands, deposited preferentially closer to the coast and more clay-rich material in the deep water, including the SW South China Sea (Li, Lin, et al., 2015).

The work presented in this study improves the sediment budget of the Sunda Shelf, but we further integrate this with other studies for the surrounding areas in order to derive a more regional sedimentary delivery history. In particular, we include deposited volumes in the Gulf of Thailand (Clift, 2006), on the continental slope immediately to the east of the Sunda Shelf (Li et al., 2013), as well as the deep-water SW South China Sea (Wu et al., 2018). Sediments in the latter area are interpreted to have been supplied from the southwest and therefore likely from the same sources as the Sunda Shelf (Liu et al., 2017).

3 | RESULTS

3.1 | Regional stratigraphy

The overall shape of the basins and their infilling stratigraphy is shown by an approximately NNW–SSE oriented profile (SCSC-14) (Figure 5a) and an ENE-WSW-oriented counterpart (SCSC-20) (Figure 5c). The former shows a clear separation of the two basins with an intervening basement high. The Nam Con Son Basin is much wider (>200 km), although about the same depth as the Cuu Long Basin (ca. 70 km width imaged). Brittle faulting can be seen cutting through the stratigraphy at least up to the top of the Middle Miocene horizon, which represents the effects of the major DRU inversion event. The older deposits are thicker within the basin centres and onlap

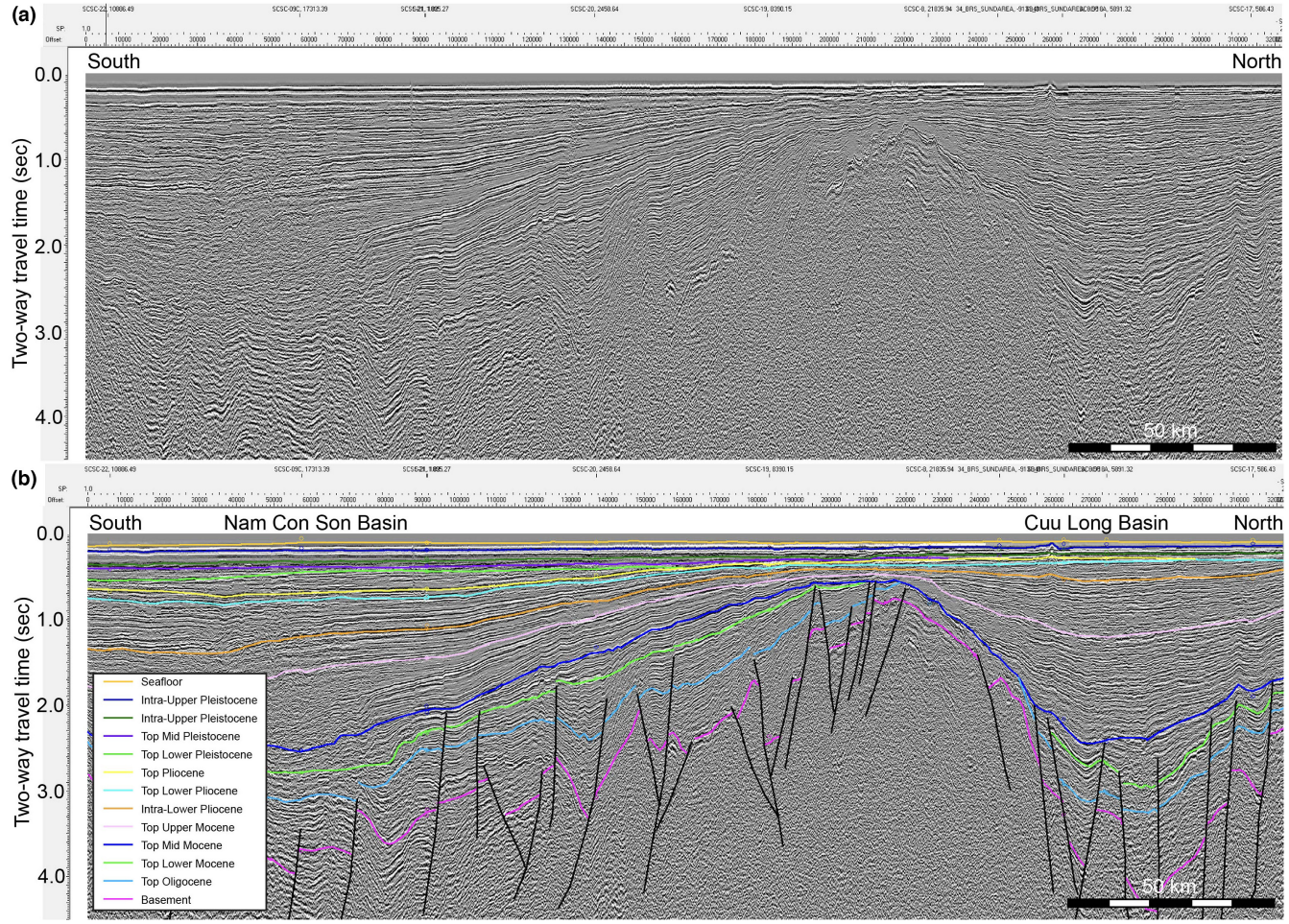

FIGURE 5 Examples of seismic reflection data spanning the Sunda Shelf. Two lines are shown roughly oriented north–south (SCSC-14) (a and b) and east–west (SCSC-20) (c and d), with both raw data and interpreted sections shown for comparison. The coloured reflectors represent regionally interpreted horizons with the age control derived by correlation to the drill sites shown in Figure 1.

onto the central high. The youngest deposits (Pleistocene-Recent) are found preserved across the entire continental shelf and are generally thin, flat-lying and gradually thicken to the south. In contrast, the older deposits above the DRU reflector are much thicker in the basin centres, and thin but do not fully pinch out, across the basement high (at least on profile SCSC-14) (Figure 5b). Below the Middle Miocene DRU unconformity, Lower Miocene and Oligocene horizons are seen to truncate against this, indicating erosion. It is noteworthy that the pre-Oligocene basement never intersects the unconformity, showing that this was not exposed at that time. Indeed, while there is clearly uplift and erosion in the Middle Miocene, much of the older stratigraphy was still preserved.

Profile (SCSC-20) (Figure 5c) provides a representative image of the basin structure in the WSW-ENE direction. Again, the DRU is prominent and remains flattish, although undulating under much of the shelf before deepening markedly to the east. The younger sediments above the unconformity thicken towards the east, so that the modern eastern edge of the shelf is underlain by a fanning array of sediments that are formed as the shelf edge prograded, largely since the Pliocene (Figure 5c,d). The westward thinning and pinching out of younger strata is very pronounced after the Early Pliocene. The Upper Miocene–Lower Pliocene thickens to the east but is also preserved in significant thicknesses across the central and western shelf. In contrast, some of the mid-Pliocene to recent sediments that underlie the shelf edge is not found under the central or western parts of the continental shelf.

This profile also highlights the complexity of structure under the Middle Miocene DRU. There is substantial variation across the shelf. In some places, the basement comes quite close to the unconformity, although the fact that many Lower Miocene to Oligocene horizons can be traced across these basement highs suggests that these were paleo-highs formed during the initial rifting, rather than being the product of inversion. Brittle faulting is again seen to be quite a high angle and of the normal throw. Although the faults likely suffered some reversal, the net

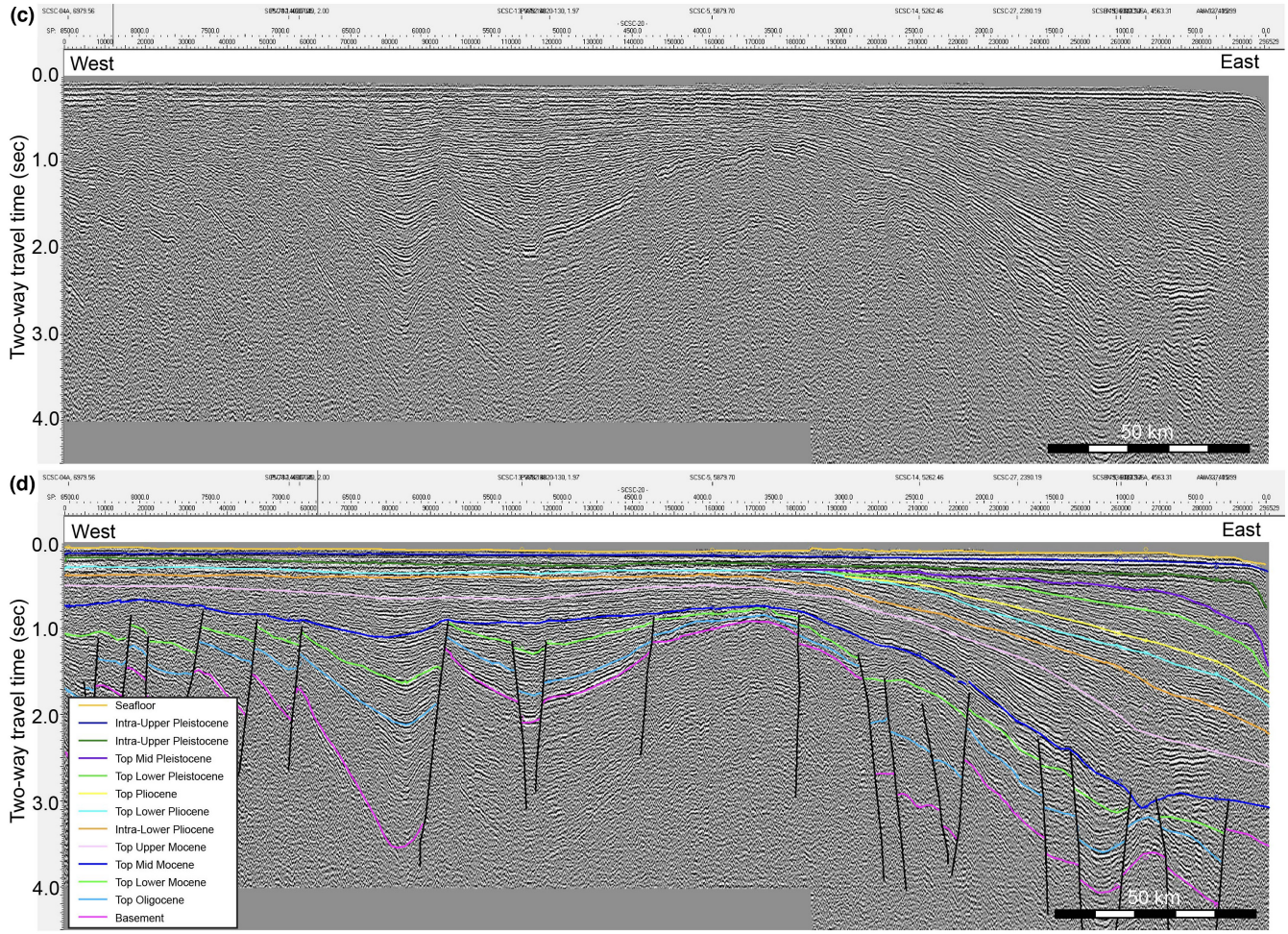

FIGURE 5 (Continued)

motion is normal, and the total amount of horizontal extension does not appear to be very large.

The changing patterns of sediment accumulation and preservation can best be appreciated across the shelf using isochore maps (Figure 6). By integrating all the interpreted lines, it is clear that during the Oligocene and Early Miocene, sedimentation mostly occurred in the central Nam Con Son Basin, although within relatively restricted deep, individual sub-basins. The Cuu Long Basin is relatively small in extent and depth at these times and the thicknesses also reduce towards the west. By the Middle Miocene this pattern had evolved slightly, with the greatest thicknesses under the central Nam Con Son Basin, but now also with two prominent depocenters along the eastern edge of the modern shelf, especially in the SE of the surveyed region. The Late Miocene, following the Middle Miocene inversion and unconformity event, shows a marked change to much more deposition in the central Cuu Long Basin and a migration towards the east in the locus of sedimentation in the Nam Con Son Basin. It is at this time that the central basement high is first clearly defined by increased subsidence in the Cuu Long Basin. Likewise, in the Pliocene, sedimentation within the Cuu Long Basin is strong, offshore what is now the Mekong Delta. Sedimentation continued throughout the Nam Con Son Basin but is very much focused under the eastern shelf edge, as seen in the reflection profiles. Finally, in the Pleistocene sedimentation was thin across the shelf but is very strong along the shelf edge, in a clearly defined wedge.

3.2 | Strain accommodation

A series of profiles can be examined to see how many extensions varied across the shelf and how the strain has been partitioned within the crust. We consider four

FIGURE 6 Isochore maps of the major stratigraphic intervals interpreted by this study. Note the appearance of a significant depocenter close to the Vietnamese coast for the (c) Upper Miocene represents the onset of Mekong Delta sedimentation. By the (a) Pleistocene almost all the sedimentation occurs on the edge of the continental shelf and slope.

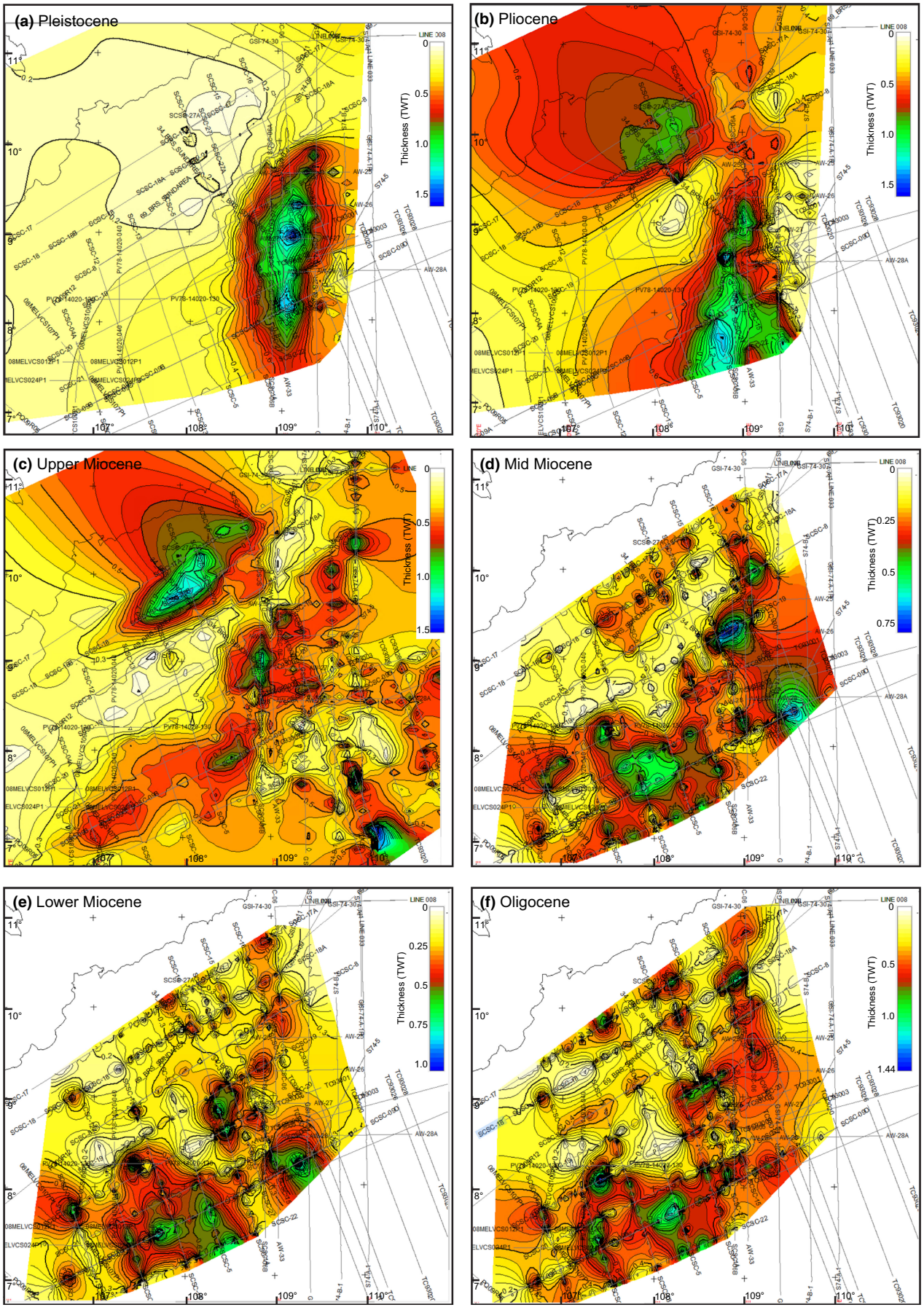

profiles as type examples, but we performed the same analysis on all profiles where the data quality permitted. Profile SCSC-20 is oriented WSW-ENE along the axis of the Nam Con Son Basin, while profiles SCSC-12, −14 and 15 lie across the strike of the basins. In order to assess the potential uncertainties introduced by our choice of Te we fully unloaded profile SCSC-15 using a range of values from Te = 3 km as the low end, through 8 and 15 km and a Te of 25 km to represent relatively stiff continental lithosphere. The results of this analysis show that although there are differences, these are generally modest (Figure 7a). The most notable exception is the structural high at around the 90–100 km mark on the profile, where uplift is ca. 600 m higher in the Te = 25 km example compared to the Te = 3 km model. This result is, however, encouraging in that it indicates that the unloaded depths to the basement are not strongly sensitive to the flexural rigidity and therefore neither is the total crustal extension estimated from those depths.

This issue can further be explored by creating a series of forward models using the measured displacement on the normal faults. We generated a synthetic section of what the basement would have looked like after the initial extension with the same range of flexural rigidities and assuming that the faulting can be used to estimate crustal extension. To undertake this assessment, we use the modelling program *Stretch*™. The four different models are shown in relation to the 8 km Te backstripped modern sediment-unloaded basement profile to see how two independent predictions compare (Figure 7b). The aim of this exercise is not to match the absolute depth but rather to see which forward model most closely matches the overall shape of the sediment-unloaded basement. The predicted basins are more angular and blocky than what is seen in the restored section. This may reflect both erosions of the basement during extension, as well as the fact that the interpretation may not have identified all the major faults. Nonetheless, the overall range of basin depths suggests

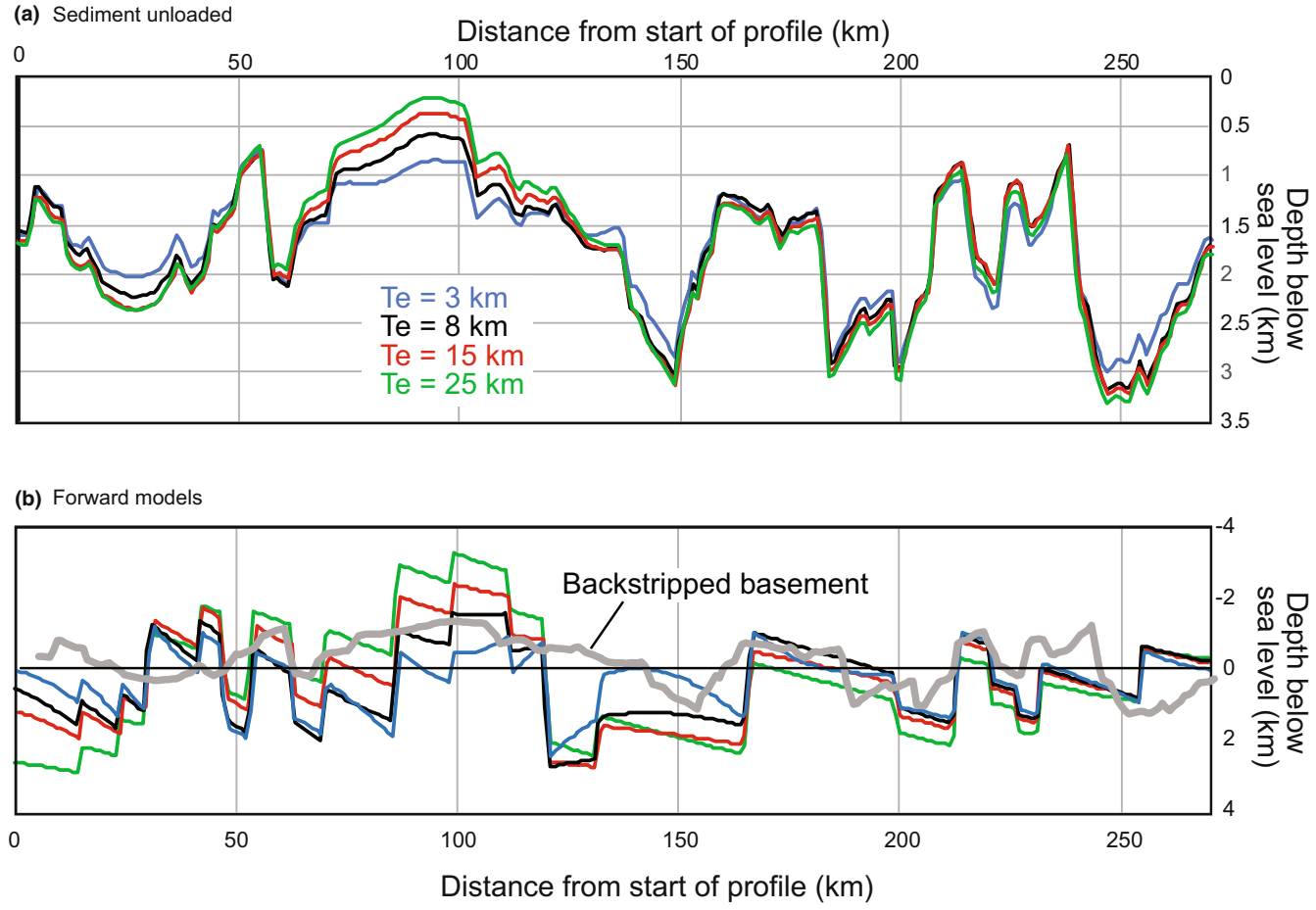

FIGURE 7 (a) Reconstructed sediment-unloaded depth to the basement along line SCSC-15, derived from *FlexDecomp* backstripping, showing the results for four different varying flexural rigidities (Te). Note that the results are quite similar but with greater topographic variation at higher Te values. (b) Forward models for predicted syn-rift topography based on the faults observed along profile SCSC-15, as predicted from the flexural cantilever model and calculated using the *Stretch* program for four different Te values. Note that the height difference between the basin centres and adjacent structural highs is much greater for high Te values, but the best match between the model and observation is found at low Te values.

that low flexural rigidity is more appropriate in this particular case. Forward models using high flexural rigidity predict basement uplift (negative depth) at the 90–100 km mark as being too high (Figure 7b), whereas the deeper sub-basins present at around 130 km are much deeper than the restored section. A better match in the overall topographical range of the backstripped basement is made with the 8 km model, which thus seems to be the most robust for basin modelling purposes.

Extension in the total crust and upper crust is determined from the modern unloaded depth to the basement and the horizontal component on the observed faults, respectively, while the lower crustal extension is then estimated from these values assuming an initial 10-km-thick brittle upper crust. The results are shown in Figure 8. In all examples, extension in the upper crust is generally rather low, a product of the high-angle character and modest throw on the faults seen in the seismic profiles. This is true whether we look perpendicular to or along the axis of the basins. In contrast, deep sub-basins within the larger depressions show substantial accommodation space, and therefore large amounts of total crustal extension. If this is not caused by faulting, then this has to be compensated for by high degrees of extension in the middle and lower crust. This depth-dependent preferential extension of the mid-lower crust is a common feature of sedimentary basins around the South China Sea (Clift et al., 2002; Davis & Kusznir, 2004). This suggests a weak lower crust that is able to deform in a ductile fashion, although this analysis does not constrain when this ductile flow would have occurred. The presumption is that much of this is associated with the initial extension of the region, starting in the Eocene–Oligocene. There does not appear to be much coupling in the extension of the upper crust, compared to the middle-lower crust, implying a detachment in the mid-crust with regard to strain accommodation.

By repeating this analysis on multiple sections, we are able to map out the extension across the basin in two dimensions. The estimates of total, upper and mid-lower crustal extension can then be interpolated and gridded using *ARCMap*™ GIS software to produce an image of the lateral variability. The overall pattern is shown in Figure 9a where the extension in the Cuu Long Basin is seen to be somewhat less than that present in the central parts of the Nam Con Son Basin. As might be expected, extension increases towards the oceanic crust east of the survey area in the deep South China Sea. If we consider differences between the upper and mid-lower crust, then the general pattern surmised from the profiles discussed above can be seen to extend across the entire survey region. Extension is clearly much higher in the mid to lower crust compared to the upper crust and it is focused on the axis of the two major basins while being moderate under the central structural height (Figure 9b). Extension is so limited in the upper crust (Figure 9c) that it is difficult to see the variations when using the same colour scale as the other maps presented here. As a result, we also show upper crustal extension with an expanded colour scale designed to highlight areas of upper crustal extension (Figure 9d). This latter map shows only moderate correspondence to the shape of the sedimentary basins seen in the seismic profiles and implies that the basins are largely a product of mid-lower crust extension and flow.

3.3 | Balancing erosion and sedimentation

Coupling between the tectonics onshore and offshore is more likely when potential erosional sources immediately juxtapose the sedimentary basins because the isostatic buoyancy forces can act more immediately over shorter distances (Clift et al., 2015; Westaway, 1994). Because we have an estimate of the rates of total sediment supply stretching from the Gulf of Thailand into the deep water of the South China Sea, it is possible to compare these with the rates of erosion reconstructed onshore by thermochronometry measurements of the bedrock sources. We consider all the basins together, as they might have been filled by supply from the same source or river. It is possible that much of the sediment came from one or two large river systems, for example, via the Mekong and its potential previous route along what is now the Chao Phraya, and into the northern part of the Gulf of Thailand before avulsing into its present position around 8 Ma (Liu et al., 2017). Thermochronometry suggests that major incision of the upper Mekong dates from ca. 17 Ma after which sediment supply might be expected to have increased. Depending on the location of the delta, the Mekong could conceivably have been a major source of sediment to the Sunda Shelf at 17 Ma (Nie et al., 2018).

Detailed provenance studies would be useful in determining whether the basins were all filled with sediment derived from one or two distant sources or whether they instead reflect erosion of unique local source terrains. Provenance analysis would be effective because the bedrock geology of Southeast Asia is subdivided into a number of tectonic units (Figure 2), each with its own unique magmatic and chemical history that may be transferred to the eroded sediments and then identified in the preserved siliciclastic sedimentary rocks of Sunda Shelf. Though there is some evidence that much of central Sundaland was exposed until the Pleistocene (Sarr et al., 2019), and we observed reduced or absent Pliocene-Recent strata in this study, it is clear that there has been some subsidence in the central part of the Gulf of Thailand (Fyhn et al., 2010). In contrast, Indochina, and especially the

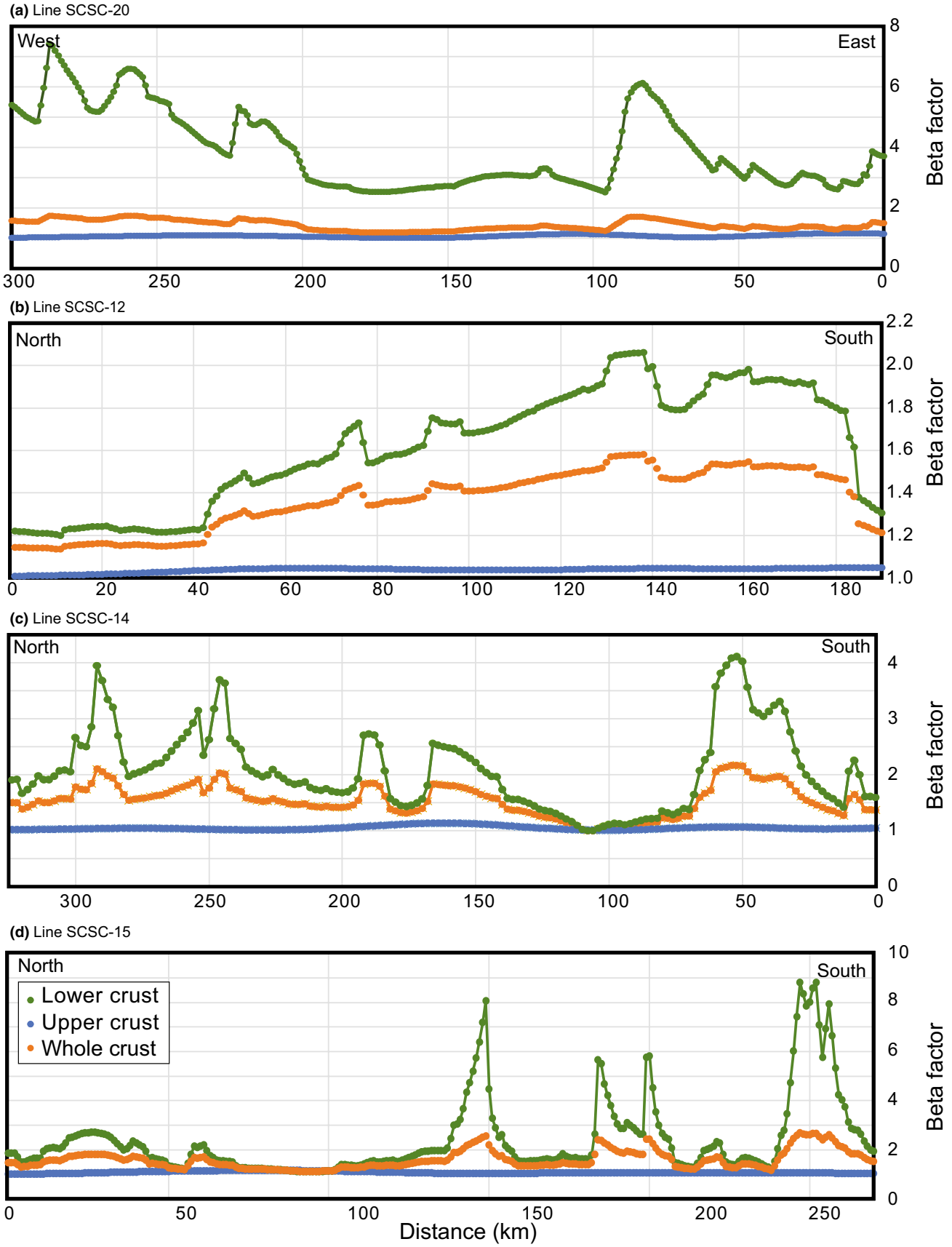

FIGURE 8 Plots show variation in the degree of upper, lower and total crustal extension along four profiles crossing the Sunda Shelf (SCSC-12, -14, -15 and -20). Note that the degree of lower crustal extension is always significantly in excess of that seen in the upper crust. See Figure 1 for the location of these profiles.

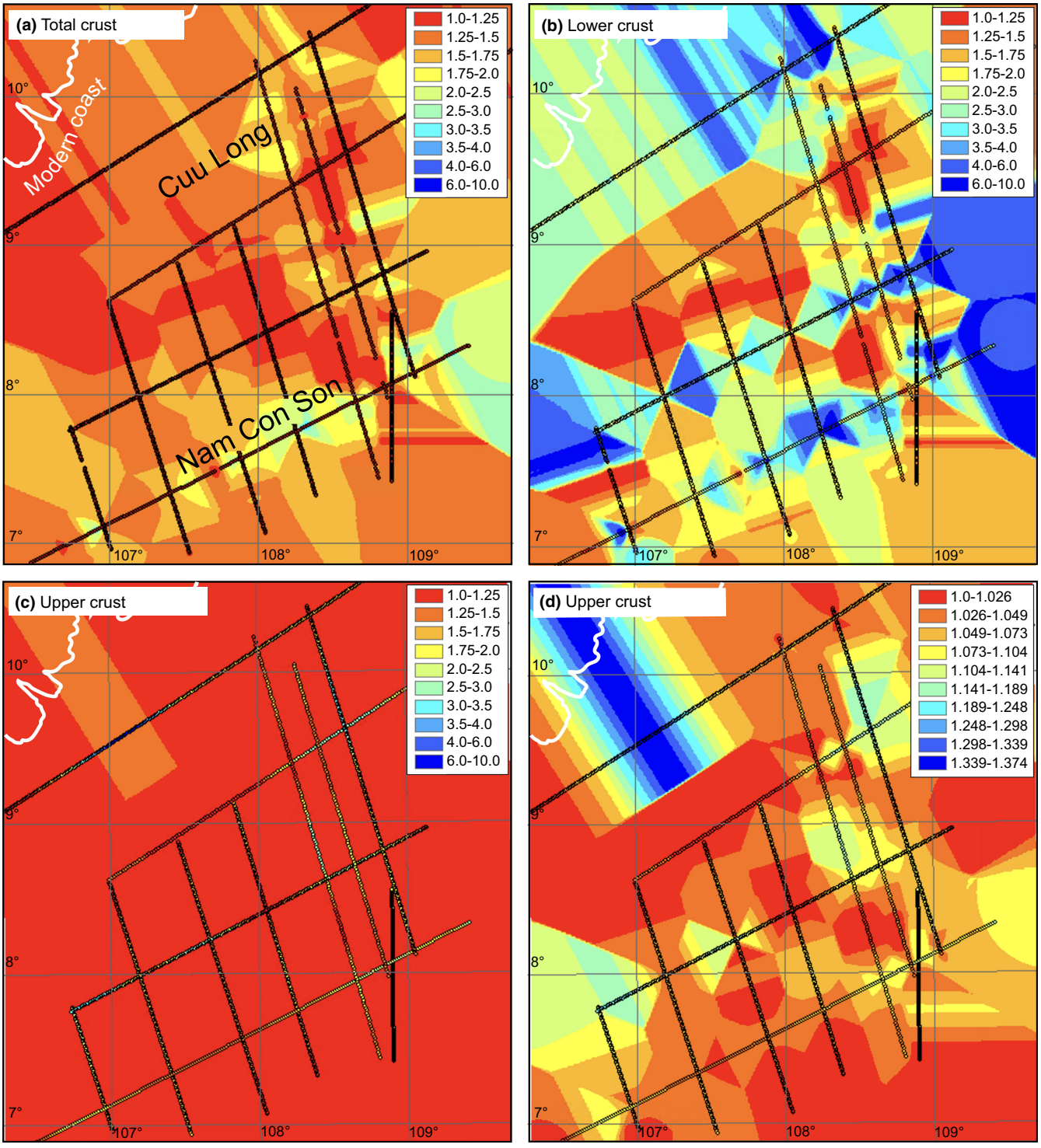

FIGURE 9 Maps showing the lateral variations in extension in (a) the total crust, (b) lower crust and (c) upper crust based on the seismic profiles shown as black lines. (c) Shows the upper crustal extension with the same colour scale as the lower and total crustal maps, whereas (d) shows the upper crustal extension with an enhanced colour scale in order to demonstrate variations in brittle faulting across the area.

Malay Peninsula, remained as highlands on either side of the basins. Sources therefore must dominantly lie outside the basins themselves, rather than from intra-basin highs.

Drainage systems have been flowing from north to south in the Gulf of Thailand since the Paleogene (Alqahtani et al., 2017; Morley & Morley, 2013; Morley & Racey, 2011) as well as towards the northeast on the Sunda Shelf offshore southern Vietnam. Recent work on detrital zircon U–Pb dates from the Cuu Long Basin indicates sediment largely from neighbouring Indochina basement until the Early Miocene, followed by supply from a paleo-Mekong (Breitfeld et al., 2022). The Nam Con Son Basin appears

to have been supplied from erosion flux from the north as well as from the rift flanks until the Early Miocene (Hall & Morley, 2004) followed by a change to supply by erosion of the Malay and Thai peninsula (Breitfeld et al., 2022). The basins that we consider were likely filled by sediments eroded from either side of the Gulf of Thailand, the catchment of the modern Chao Phraya, or from coastal Vietnam-Cambodia. Although there is evidence for Neogene uplift and erosion in Borneo (Hutchison et al., 2000) and the southern Malay Peninsula (Cottam, Hall, & Ghani, 2013; Kassa et al., 2019), these sources seem less important as their erosional products would have been preserved in the southern basins of Sundaland (i.e. the Penyu, West Natuna and Luconia basins), based on a general understanding of regional drainage patterns, and consistent with the detrital zircon data (Breitfeld et al., 2022).

Exhumation around Sundaland is generally not very deep, except in limited areas linked to fault zones (e.g. the Three Pagodas Fault Zone, Figure 2) and the Doi Inthaonon area on the west side of the Chiang Mai Basin (Morley, 2015) where erosion of the footwall has contributed to the fill of the adjacent basin. The erosional history of the potential sources can be best constrained through cooling histories reconstructed from low-temperature zircon and apatite fission track methods. These measure the cooling of bedrock from 230–250°C to 60–110°C respectively (Donelick et al., 2005; Gallagher et al., 1998). Shallower exhumation can be tracked with the (U–Th)/He method, also applied to apatite and zircon (Reiners, 2005). Rough estimates of the eroded rock volumes can be generated by using a continental geothermal gradient and knowing the area of the exhuming terrain, as shown in Figure 2. Madon (1997) recorded an average heat flow of 33–42 mW/m^2 in the Malay Basin, equivalent to a gradient of 23–30°C/km. A regional compilation (Southeast Asian Research Group, 2022) shows higher geothermal gradients (100–120 mW/m^2, 71–85°C/km) over the southern Malay Peninsula and Cambodia. In western Borneo and SE Vietnam (over the Central Highlands), geothermal gradients are also elevated (90–100 mW/m^2, ca. 67°C/km). They are moderately higher in Peninsular Thailand (70–80 mW/m^2, ca. 60°C/km). Heat flow values lie close to the continental average (30°C/km) in other regions (e.g. Thailand). Applying these gradients to the thermal histories of the bedrock allows a rough estimate of erosion from each of the major sources to be derived (Table 2). For example, with a mean 16.4 Ma apatite U–Th/He age in Peninsular Thailand (Sautter et al., 2019) we infer 60°C of cooling since 16.4 Ma (Ehlers & Farley, 2003). Because the geothermal gradient in this area is ca. 60°C/km this means that ca. 1 km of erosion has taken place since 16.4 Ma, over an area of 120,000 km^2. This implies a long-term average erosion rate of 0.061 km/m.y. and thus the erosion of 116,854 km^3 of bedrock since 15.97 Ma (base of the Middle Miocene). Because of a lack of regional coverage, we must assume uniform exhumation over the entire area of the tectonic block. If more than one thermochronometer is available for a single block then an adjustment was made to reflect changes in cooling/erosion rate.

Thermochronologic data from the Malay Peninsula are from Krähenbuhl (1991), Cottam, Hall, and Ghani (2013) and Kassa et al. (2019), while constraints from peninsular Thailand are from Upton (1999) and Sautter et al. (2019). Upton (1999) also provides regional control over much of Thailand, but with additional detail in SE Thailand derived from Nachtergaele et al. (2020) (see Figure 2 to show where specific areas are located). Carter et al. (2000) supply thermal models for southern Indochina, with Fyhn et al. (2016) adding constraints from Cambodia. Erosion in Sabah (Mt. Kinabalu region) and in Sarawak are measured by Cottam, Hall, Sperber, et al. (2013) and Hutchison et al. (2000), although the sediment derived was not preserved in the northern Sundaland basins we study here. The simplified cooling histories for the potential source regions are shown in Figure 10. By applying the estimated geothermal gradient for each tectonic block to its cooling history reconstructed from the thermochronology, we can convert the cooling to an erosion history. When attempting to compare the eroded (derived from the cooling history of the source terrains and their extent) and deposited volumes (derived from seismic interpretation and after accounting for sediment porosity (Sclater & Christie, 1980)) we presume that half the sediment eroded from peninsular and western Thailand is transported west into the Andaman Sea, with the other half deposited in the Gulf of Thailand. We have no way of knowing exactly how much eroded sediment is transported east rather than west but there is no reason to think that all the eroded sediment was transported to each side of the peninsular and so a 50:50 split was employed to provide a rough estimate for how much sediment might be expected, given the roughly central location of the modern drainage divide. In the present day ca. 45% of the peninsular drains west in the Andaman Sea and 55% into the Gulf of Thailand. In each source terrain, we calculate the weight of eroded rock by converting eroded bedrock volumes using an average density of 2700 kg/m^3. Thus, by knowing the area, rate and duration of exhumation the total mass of eroded material may be estimated. The results for each block are provided in Table 2.

4 | DISCUSSION

4.1 | Patterns of sedimentation

Because the Upper Miocene to Recent sediments is relatively thin, or even absent, on the western side of the surveyed region (Figures 5 and 6), older deposits dominate the

TABLE 2 Estimates rates of erosion for different time periods and the associated eroded bedrock volumes for each of the potential source areas considered to have supplied the eastern Sunda Shelf since the Oligocene.

	Mount Kinabalu		Sarawak Rajang		Peninsula Thailand		Western Thailand	
Age (Ma)	**Erosion rate (km/my)**	**Amount eroded (km^3)**	**Erosion rate (km/my)**	**Amount eroded (km^3)**	**Erosion rate (km/my)**	**Amount eroded (km^3)**	**Erosion rate (km/my)**	**Amount eroded (km^3)**
0	0.170		0.100		0.061		0.159	
2.58	0.170	13,597	0.100	31,218	0.061	18,878	0.159	41,130
5.33	0.170	14,493	0.100	33,275	0.061	20,122	0.159	43,841
11.63	0.830	162,099	0.100	76,230	0.061	46,098	0.159	100,435
15.97			0.046	24,064	0.061	31,756	0.159	69,188
23.03			0.046	39,145	0.043	36,020		
33.9			0.046	60,270	0.043	55,459		
Total		**190,188**		**264,202**		**208,333**		**254,594**
Area		31,000		121,000		120,000		100,000
Source reference	Cottam, Hall, and Ghani (2013)		Hutchison et al. (2000)		Sautter et al. (2019), Upton (1999)		Upton (1999)	

	SE Thailand		Eastern Thailand		Southern Indochina		Cambodia	
Age (Ma)	**Erosion rate (km/my)**	**Amount eroded (km^3)**	**Erosion rate (km/my)**	**Amount eroded (km^3)**	**Erosion rate (km/my)**	**Amount eroded (km^3)**	**Erosion rate (km/my)**	**Amount eroded (km^3)**
0	0.087		0.122		0.111		0.031	
2.58	0.087	4936	0.122	17,620	0.111	16,829	0.031	2444
5.33	0.087	5261	0.122	18,780	0.111	17,938	0.031	2605
11.63	0.087	12,052	0.122	43,024	0.068	25,192	0.031	5968
15.97	0.087	8303	0.122	29,639	0.054	13,848	0.031	4111
23.03	0.253	39,222	0.050	19,844	0.046	19,225	0.031	6687
33.9	0.359	85,845	0.046	27,719	0.042	26,684	0.031	10,296
Total		**155,619**		**156,627**		**119,716**		**32,111**
Area		22,000		56,000		59,000		31,000
Source reference	Nachtergaele et al. (2020)		Upton (1999)		Carter et al. (2000)		Fyhn et al. (2016)	

TABLE 2 Continued

	Peninsula Malaysia		Grand total (not including Borneo and Peninsula Malaysia)				
Age (Ma)	Erosion rate (km/my)	Amount eroded (km^3)	Total amount eroded (km^3)	Total amount eroded (Mt)	Erosion rate (Mt/y)	Maximum	Minimum
0	0.078						
2.58	0.078	26,508	101,837	275	107	128	85
5.33	0.078	28,255	108,547	293	107	128	85
11.63	0.056	45,921	232,769	628	100	120	80
15.97	0.043	24,723	156,845	423	98	117	78
23.03	0.026	23,898	120,998	327	46	56	37
33.9	0.098	140,183	206,004	556	51	61	41
Total		289,489	**1,140,946**	**3081**			
Area		131,000					
Source reference	Cottam, Hall, Sperber, et al. (2013), Krähenbuhl (1991), Kassa et al. (2019)						

sediments preserved in that area, while the reverse is true towards the east. This pattern implies that much of the subsidence and sediment preservation in the west occurred early in the basin history. Only limited amounts of further subsidence occurred in the Late Miocene to the present, limiting the amount of sediment that may have been preserved in this western area. Any additional sediment reaching that part of the shelf would have bypassed eastwards into deeper water. In contrast, the thicker, younger deposits in the east reflect the significant accommodation space available on the edge of the Sunda Shelf reflecting the high degrees of extension and subsidence achieved in proximity to the continent–ocean transition. The basins under the modern Sunda Shelf are full of sediment and the region is not experiencing rapid tectonic subsidence, which is why the Pleistocene sedimentation has largely been along the eastern edge of the shelf (Figure 6). This pattern began in the Pliocene, but at that time, there was more accommodation space in the Cuu Long Basin where a good deal of sediment from a paleo-Mekong River was sequestered (Breitfeld et al., 2022).

The sedimentation patterns tell us something about the history of the Mekong River, which implies sediment delivery from the north and is consistent with the detrital zircon data (Breitfeld et al., 2022). The first indication of rapid sedimentation in the north of the surveyed area comes in the Late Miocene. There is a large depocenter close to the modern Mekong River mouth at that time and in the subsequent Pliocene (Figure 6). The lack of earlier sedimentation does not preclude sediment supply from the north at this time, as suggested by Breitfeld et al. (2022), only a lack of accommodation space. The onset of rapid sedimentation in the Late Miocene in the Cuu Long Basin is consistent with sediment geochemical data from the South China Sea, pointing to the initiation of the modern Mekong in its present position starting ca. 8.5 Ma (Liu et al., 2017). However, this is later than the establishment of the 'Paleo-Mekong 2' in this location in the Middle Miocene, as proposed Breitfeld et al. (2022). We note that sedimentation in the Cuu Long Basin did increase in the Middle Miocene, before reaching a maximum in the Late Miocene. It is possible that if a 'Proto-Chao Phraya' (consisting of the modern river connected to the upper reaches of the modern Mekong) had been supplying sediment to the Gulf of Thailand before the Middle Miocene, then this may have been the source of some of the sediment found in the Nam Con Son Basin at that and earlier times. This would have been supplied largely from the west of the studied area.

4.2 | Sediment mass balancing

The potential influence of an older Proto-Chao Phraya extending as far as the SE Tibetan Plateau can further be

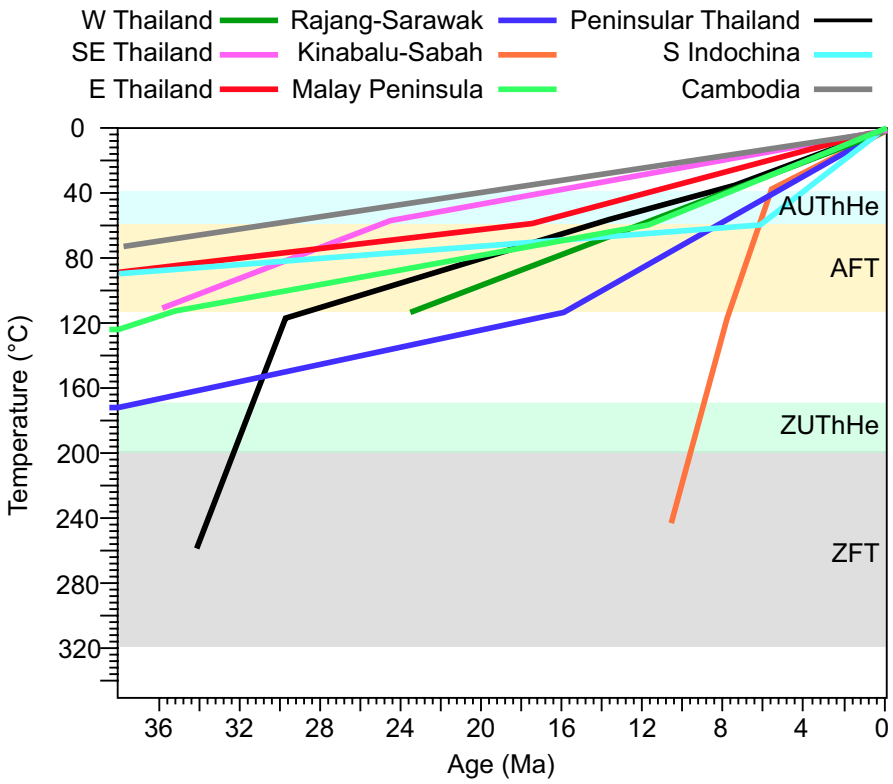

FIGURE 10 Simplified cooling histories of the potential source terrains supplying sediment to the Gulf of Thailand and Sunda Shelf. Kinabalu-Sabah is from Cottam, Hall, Sperber, et al. (2013), Rajang-Sarawak is from Hutchison et al. (2000), Peninsular Malaysia is from Upton (1999) and Sautter et al. (2019), Peninsular Thailand from Sautter et al. (2019), Western Thailand is from Upton (1999), Eastern Thailand is from Upton (1999), SE Thailand is from Nachtergaele et al. (2020), Cambodia is from Fyhn et al. (2016) and southern Indochina is from Carter et al. (2000). Coloured horizontal bands show the partial annealing zones for a series of low-temperature thermochronometers. AUTheHe, Apatite U–Th/He; AFT, Apatite fission track; ZFT, Zircon fission track; ZUTheHe, Zircon U–Th/He.

tested through the sediment budget of the regional basins and the estimates of erosion from possible source areas around the Gulf of Thailand and southern Indochina. Figure 11d shows the direct comparison between the amount of rock eroded from the basement terrains that contributed to the studied basins. We reduce the eroded flux from western and peninsular Thailand by 50% because it is unrealistic to assume that all the material eroded from these sources was routed to the Gulf of Thailand. Some of the sediment likely flowed westwards into the Andaman Sea. The overall impression is that the supplied and deposited masses are within error of one another. However, during the Late Miocene and Pliocene, the total eroded amount appears to exceed the deposit, implying that some of the sediment is being routed elsewhere at that time, or that the uncertainties in cooling histories are greater than assumed. The fact that the local bedrock appears to be capable of filling the basins in northern Sundaland is somewhat surprising. It implies a little role for additional supply from a major Asian river system, sourcing much further north within the Tibetan Plateau, that is Paleo-Mekong 2 (Breitfeld et al., 2022).

Clearly, we know that the Mekong River has been contributing sediment into the area, possibly since the Middle Miocene and definitely since ca. 8.5 Ma (Li et al., 2013; Liu et al., 2017). However, the Late Miocene is a time when the deposited volumes are estimated to have been smaller than the local erosion, meaning that some of the Paleo-Mekong 2 sediments are being stored elsewhere, possibly further north under onshore Indochina. There is no need to invoke the influence of sources located far from SE Asia in accounting for the filling of the Sundaland basins. Although Breitfeld et al. (2022) propose that drainage may have come from as far as the "Himalayas" (but presumably SE Tibetan Plateau), that study also notes that erosion of Sibamasu might also be consistent with the zircon dates found in the sediments. If that was true there is no need to propose supply from a Proto-Chao Phraya coming from the Tibetan Plateau into the Gulf of Thailand since the Oligocene to account for the sedimentary fill, consistent with the earlier analysis of Hall and Morley (2004). Thermochronology evidence from the SE Tibetan Plateau does indicate incision and erosion starting in the Middle Miocene (Nie et al., 2018) and must have been delivered

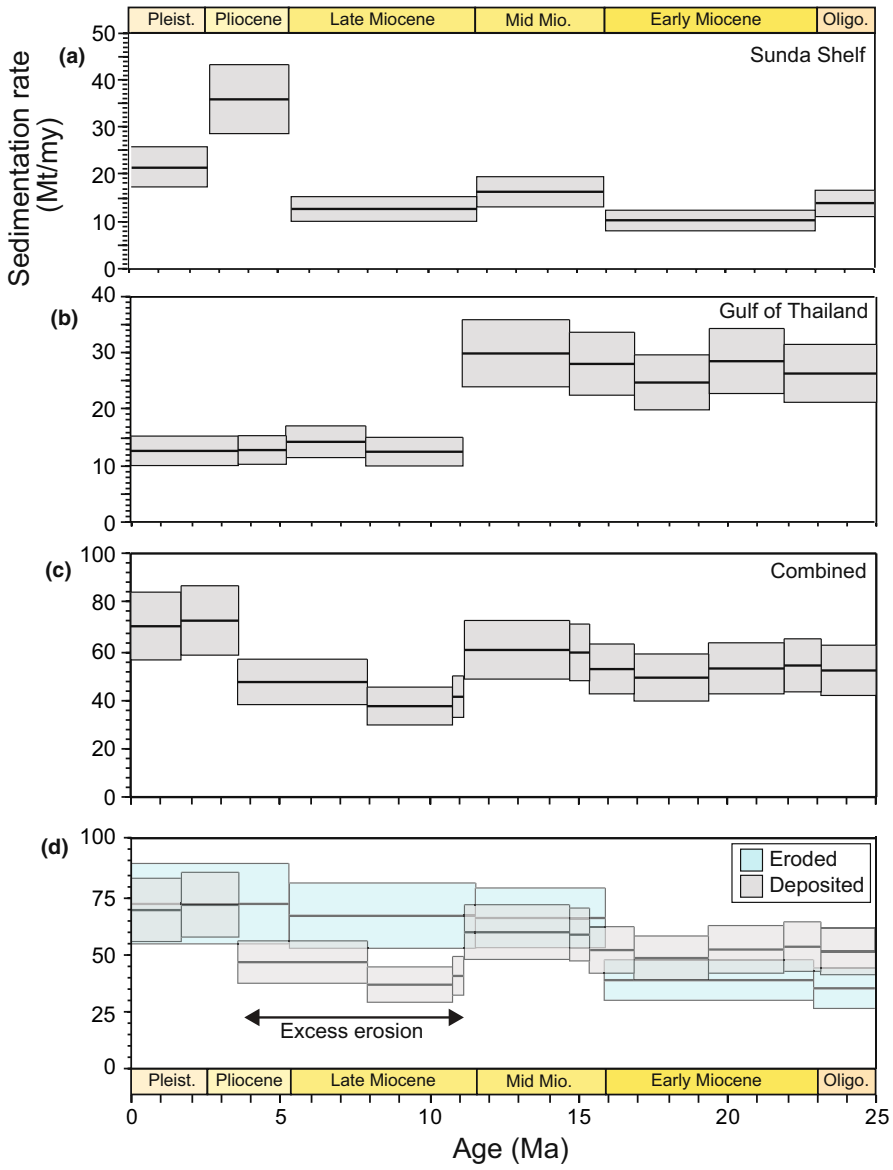

FIGURE 11 (a) Estimated sediment budget for the northern Sunda Shelf, with the grey boxes showing the uncertainties that are largely linked to the time–depth conversion from the original seismic. The heavy black line shows the average value for each time period. (b) Sediment budget for the Gulf of Thailand, including the Penyu, Malay and Pattani basins from Clift et al. (2006). (c) Integrated sediment budget for all the basins in the Gulf of Thailand and the northern Sunda Shelf, including the slope sediments documented by Li et al. (2013) and the deep-water sediments in the south-western South China Sea from Wu et al. (2019). (d) Comparison of the sediment budget for the Gulf of Thailand Sunda Shelf region and the eroded volumes estimated from the regional thermochronology of all potential source areas in Peninsula and mainland Thailand and Indochina that might be supplying sediment into the basins.

by the Paleo-Mekong 2 into the region of the Cuu Long Basin.

4.3 | Timing of subsidence

The one-dimensional subsidence analysis calculated from the drilling sites on the shelf edge shows that the time of fastest sediment-unloaded basement subsidence was in the Middle Miocene, immediately after the DRU. After ca. 10 Ma, basement subsidence continued at a slower rate (Figure 12). If we were to assume that the rapid subsidence was related to active extension, it is possible to estimate the degree of extension that would be required to generate such rates, based on a uniform extension model (McKenzie, 1978). However, it seems unlikely that this was the cause because the brittle faulting observed on the seismic profiles finished at the DRU variously dated at ca. 12–13 Ma to 16 Ma) (Morley et al., 2022). Instead, we infer that the rapid subsidence in the Middle Miocene reflects the gravitational collapse of the basins, following inversion driven by short-lived compression during the collision of Borneo and the Dangerous Grounds (Hutchison, 2005). The significant differences between these relatively closely situated boreholes reflect the fact that subsidence at a single site depends on a number of factors, not least where it lies relative to the major faults defining the basin. Thus, a drill site in the hanging wall of a normal fault would be expected to subside during active extension while one in the footwall block might show uplift. There might also be important differences in sediment loading over modest horizon distances.

A more meaningful analysis of the basement subsidence comes from a consideration of the pseudo-well estimated for the shelf edge region (Figure 12). In this case, the early syn-rift subsidence is clearly demonstrated and

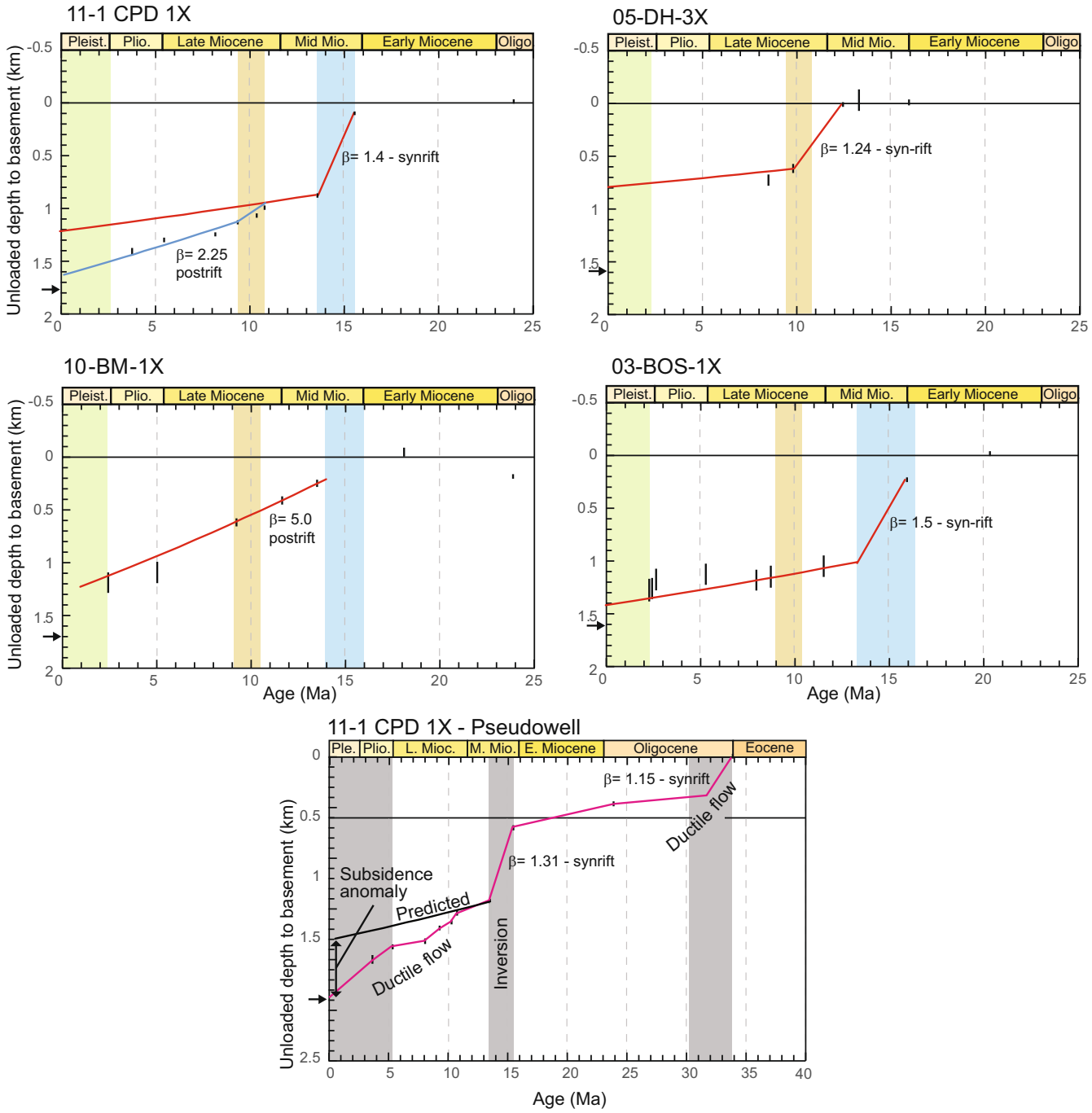

FIGURE 12 One-dimensional basement subsidence reconstructions derived from the backstripping analysis of drilled sections in oil and gas wells on the outer eastern part of the Sunda Shelf. Vertical black bars show the uncertainty of the water depth estimates. Black arrows on the left of each plot show the modern sediment-unloaded depth to the basement. Red lines show the expected subsidence assuming uniform pure shear extension, with the thermal subsidence predicted from the amount of syn-rift subsidence. Green, orange and blue vertical, coloured bars show times of accelerating subsidence interpreted as phases of extension. The pseudo-well represents an extrapolation of the drilled section, including sediment below the depth of penetration by drilling but imaged on the seismic profiles.

is dated as having occurred during the Oligocene, perhaps a little in the Late Eocene (Matthews et al., 1997). The DRU-related uplift that occurred at the start of the Middle Miocene is not reflected in the stratigraphy, except in the form of the DRU itself, and the amount of uplift is unknown. However, we note that there is a sharp, net decrease in basement depth between the start and the end of the DRU. This implies additional crustal thinning at this time and was an important part of the total subsidence. Because this is a time (ca. 16 Ma) when regional extension and seafloor spreading ceased (Li, Xu et al., 2014), it is likely that most of this extension was caused by

gravitational collapse in the aftermath of the compressional event.

The amount of extra, rapid subsidence that occurred at this time (ca. 14–16 Ma) can be used to infer how much extension may have taken place ($\beta = 1.31$ at the pseudo-well (McKenzie, 1978)). This can be compared with the reconstructed subsidence because a phase of crustal thinning might be expected to be followed by renewed post-rift thermal subsidence. Figure 12 shows that instead of gradually slowing subsidence after the inversion, the area continued to subside more rapidly than might be expected from a simple uniform extension model. The basement subsided more rapidly after than before the DRU. The disparity between the expected subsidence record, and that reconstructed means that we have as much as 500 m of additional sediment-unloaded subsidence in the pseudo-well than would be expected. It is noteworthy that the discrepancy between the reconstruction and the projected subsidence mostly occurred after 10 Ma and especially since the onset of the Pliocene. This was a time when loading of the shelf edge area was at its greatest during the formation of the shelf edge clinoforms (Li et al., 2013), as well as during the loading of the Cuu Long Basin by sediment delivered from the Paleo-Mekong River 2. The faster post-rift subsidence does not correlate with any brittle upper crustal deformation that can be seen in the seismic profiles and implies thinning by the mid-lower crustal flow.

4.4 | Strain accommodation

The mid-lower crust is always more extended than the upper crust (Figure 9), and this observation indicates a mass balance problem. If more mid-lower crust is lost from the area than from the upper crust, then where does this additional material go? Previous studies have suggested that the ductile material would flow towards the extended oceanic crust if the flow was related to break up (Clift et al., 2002; Huismans & Beaumont, 2011). Because this area lies in front of a now-defunct seafloor spreading centre (Huchon et al., 2001), we know that the mid-lower crustal loss must have preceded the final break-up. This implies that the ductile crust must have flowed towards the northeast, towards the oceanic crust and prior to final break-up. The only alternative is that the ductile crust flowed towards the north under Indochina. This is not likely because the thicker crust present under that region would favour flowing away from this area because of density and gravitational potential considerations (Clark & Royden, 2000), at least during the time of active extension (McKenzie et al., 2000). What is clear is that extension under the Sunda Shelf is not uniform in character and requires ductile flow to account for the subsidence. This is consistent with the idea that this crust was hot and weak prior to the onset of active extension and contrasts with models that treat Indochina as a rigid block (Replumaz & Tapponnier, 2003; Tapponnier et al., 1982). Much of this crustal flow must have occurred during Oligocene active extension. However, the subsidence history shown by the one-dimensional analysis (Figure 12) indicates that some of this flow occurred in the Late Miocene–Pliocene, following basin inversion, and subsequent collapse when there were no regional extensional stresses.

We now investigate whether there might be coupling between erosion onshore and the ductile flow under the Sunda Shelf basins by examining the history of sedimentation in the basins and erosion onshore. Models that have favoured a coupling between the two invoke landward flow of ductile, low-viscosity mid-lower crust (Clift et al., 2015; Dong et al., 2020; Morley & Westaway, 2006; Westaway, 1994). This mechanism might be applicable to account for the patterns of extension reconstructed here.

4.5 | Climate-tectonic interactions

In order to understand how climate might be affecting erosion and tectonics in the Sunda Shelf region, we have to compare the subsidence records, reconstructed here, with regional and global climate records. The peak in sedimentation in the Sunda Shelf, which we see in the Pliocene, correlates with the time of strengthening summer monsoon rains in southern China (Figure 13b). In SE Asia (SW South China Sea), the Pliocene was a time of increasing haematite/goethite values in South China Sea sediment (at IODP Site U1433 and ODP Site 1143) (Liu et al., 2019).

FIGURE 13 Synthesis diagram comparing some of the results from this work with regional tectonic and climatic events. (a) Normalized sedimentation rates for the Sunda Shelf. (b) Haematite/goethite values from ODP Site 1143, as a proxy for humidity in Indochina from Liu et al. (2019). (c) C_{RAT} monsoon proxy for clay mineralogy based on spectral data from the northern South China Sea from Clift, Hodges, et al. (2008). (d) Global compilation of oxygen isotopes from benthic foraminifers, as a proxy for average ocean water temperatures from Westerhold et al. (2020). (e) Mean global sea level from Miller et al. (2020). (f) Tectonic events in Southeast Asia that may have influenced sedimentation on Sunda Shelf. Vietnamese exhumation from Carter et al. (2000), Central Highland Flood Volcanism from Hoang and Flower (1998), Malaya Basin inversion age from Madon and Watts (1998), motion on the Red River Fault Zone (RRFZ) from Gilley et al. (2003). DRU, Deep Regional Unconformity (Morley, 2016). End of the seafloor spreading in the South China Sea from Li, Xu et al. (2014). Subsidence events are coloured blue as defined by this study.

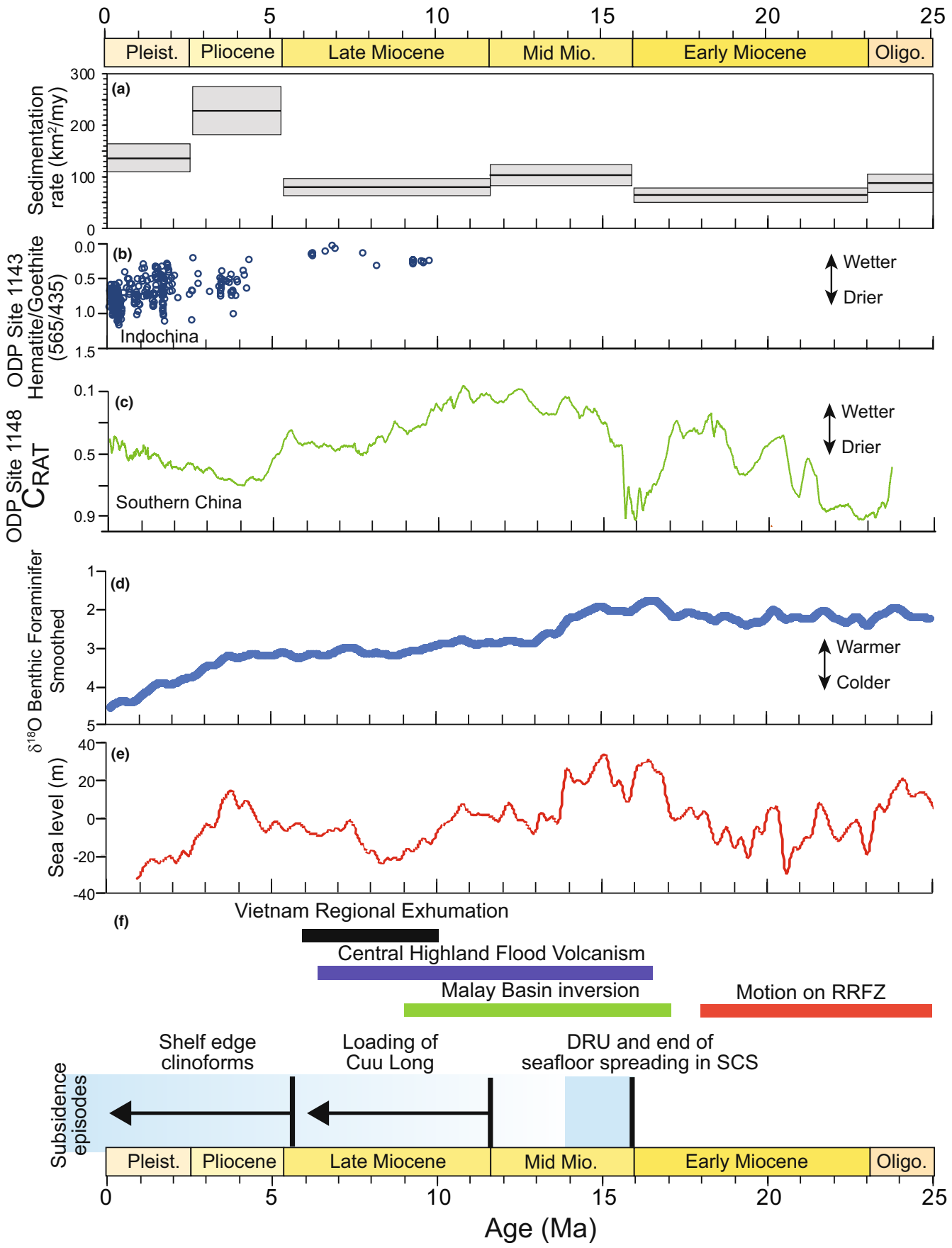

This is associated with drier or more seasonal conditions in the Mekong Basin of Indochina (Liu et al., 2019; Miao et al., 2017). However, most sediment in the river is eroded from the upper reaches where the climate is more like that of southern China (Clift et al., 2014). It is therefore possible that the faster sediment accumulation in the Pliocene is linked to heavier rains in the upper Mekong in SE Tibet.

The source bedrock thermochronology around the Sunda Shelf does not highlight this as a time of faster exhumation locally, but the depths of unroofing are not that great and this may not be resolvable. An exception is the Central Highlands of Vietnam where rapid cooling started just before the increase in sedimentation rate, most notably in the adjacent Cuu Long Basin (Figure 6). Numerical modelling has demonstrated that sediment loading may cause ductile mid-lower crustal flow to occur (Clift et al., 2015; Morley & Westaway, 2006). We suggest that some of the preferential thinning seen in the Cuu Long Basin may be related to the fast Pliocene sedimentation. Some of the mid-lower crust probably flowed northwards under southern Indochina, and back towards the exhuming Central Highlands. Some of the flow may also have been directed to the west where the amount of Plio-Pleistocene subsidence is very low. Modest crustal thickening could account for the pinching out of sedimentary packages developed on the continental shelf in a westerly direction. The loading of the offshore basins coupled with onshore uplift alters the pressure gradient to allow some reverse flow during the post-rift period.

Rapid exhumation in the Central Highlands postdated the emplacement of flood basalts in this region when the area was uplifted. Rapid sedimentation on the eastern edge of the shelf is also within the Plio-Pleistocene and may be responsible for some of the ductile deformation. This is generally a time of cooling climate (Figure 13d), but it is not clear why erosion might have increased as a result of this shift except for in the Central Highlands. However, falling sea levels (Figure 13e) would act to increase erosion. We argue that changes in erosion and in sediment loading are mostly driven by regional climate changes associated with the Asian monsoon system and that have been reconstructed since the Oligocene using weathering proxies and palynology in the South China Sea (Clift et al., 2014; Liu et al., 2019). Although the Oligocene extension is related to regional extensional tectonics, and correlates with seafloor spreading in the South China Sea, it is not clear that later subsidence events are linked to regional solid Earth stresses.

5 | CONCLUSIONS

The eastern Sunda Shelf is underlain by two large sedimentary basins, the Cuu Long and Nam Con Son basins. These formed largely as a result of regional extension in front of seafloor spreading centre propagating towards the Southwest during the Oligocene-Early Miocene (Barckhausen et al., 2014; Li, Xu et al., 2014). A crustal extension was non-uniform, with greater extension in the ductile mid-lower crust compared to the brittle upper crust. Lower crust is inferred to have flowed towards the continent–ocean boundary to the northeast. Sediment was supplied to the basins from the surrounding basement highs in Indochina, Peninsular and mainland Thailand, and was ponded close by. Following the collision of the Dangerous Grounds block with Borneo at ca. 16 Ma (Clift, Lee, et al., 2008; Hinz & Schlüter, 1985; Hutchison, 2005), the basins were inverted and partly eroded during a compressional period. The extensional collapse of the inverted basins was followed by a time of accelerated subsidence that was especially marked after ca. 10 Ma and correlated with a phase of significant sedimentation. Although the rapid erosion and sediment supply occurred at a time of stronger summer monsoon in South China environmental proxies suggest that this was a drier time in Indochina, indicative of a northerly migration of the Intertropical Convergence Zone at that time (Liu et al., 2019). The wet upper reaches of the Mekong were important sediment suppliers and experienced faster erosion driven by strong summer rains.

Emplacement of the Central Highland volcanic field in Vietnam provided an important source of sediment during the Late Miocene, with large volumes concentrated in the northern Cuu Long Basin. The sediment loading, coupled with erosion and isostatically driven uplift onshore drove enhanced ductile mid-lower crust flow. This was largely directed towards the north under Indochina from across the entire shelf, but especially from under the basin depocenters and the shelf edge. The accelerated subsidence seen in the eastern shelf continued to the present day and represents a form of climate–tectonic coupling in which climate change drives exhumation in one location and loading in another, fostering ductile crustal flow. In contrast, Upper Miocene-Recent sedimentation is very condensed in the western and central parts of the surveyed region with most sediment accumulating in clinoforms along the shelf edge after filling of the Cuu Long Basin. The sediment is partly supplied by the Mekong River, whose delta has occupied its present location at least since the Late Miocene (Breitfeld et al., 2022; Liu et al., 2017). Regionally, there is little need for major sediment supply from a river deriving material from the Tibetan Plateau to account for the sediment volumes in the basins. Nonetheless, the Mekong is a significant factor at the present time. We find little evidence for a strong influence of an enlarged paleo-Chao Phraya River in supplying sediment to the study region.

ACKNOWLEDGEMENTS

We thank Alan Roberts, Nick Kusznir and Andy Alvey for use of the software *FlexDecomp* and *Stretch*. IHS Markit is thanked for the licence granted to LSU for the academic use of their *Kingdom* software. Gérôme Calves, Long Van Hoang and Vashan Wright are thanked for their help with *Kingdom*. The project was supported by the Charles T. McCord Chair in Petroleum Geology and completed during PC's study visits to the Hanse Wissenschaftskolleg (Germany) and the University of Hong Kong. The study was designed by PC. PC and LW did the interpretation and analyses together and both contributed to the writing of the manuscript.

CONFLICT OF INTEREST STATEMENT

There is no conflict of interest.

PEER REVIEW

The peer review history for this article is available at https://www.webofscience.com/api/gateway/wos/peer-review/10.1111/bre.12809.

DATA AVAILABILITY STATEMENT

Research data are not shared.

ORCID

Peter D. Clift https://orcid.org/0000-0001-6660-6388

REFERENCES

Alqahtani, F. A., Jackson, C. A.-L., Johnson, H. D., & Som, M. R. B. (2017). Controls on the geometry and evolution of humid-tropical fluvial systems: Insights from 3D seismic geomorphological analysis of the Malay Basin, Sunda shelf, Southeast Asia. *Journal of Sedimentary Research*, *87*(1), 17–40. https://doi.org/10.2110/jsr.2016.88

An, A. R., Choi, S. H., Yu, Y., & Lee, D.-C. (2017). Petrogenesis of late Cenozoic basaltic rocks from southern Vietnam. *Lithos*, *272-273*, 192–204. https://doi.org/10.1016/j.lithos.2016.12.008

Barckhausen, U., Engels, M., Franke, D., Ladage, S., & Pubellier, M. (2014). Evolution of the South China Sea: Revised ages for breakup and seafloor spreading. *Marine and Petroleum Geology*, *58*, 599–611. https://doi.org/10.1016/j.marpetgeo.2014.02.022

Bott, M. H. P. (1992). Passive margins and their subsidence. *Journal of the Geological Society*, *149*(5), 805–812. https://doi.org/10.1144/gsjgs.149.5.0805

Braitenberg, C., Wienecke, S., & Wang, Y. (2006). Basement structures from satellite-derived gravity field: South China Sea ridge. *Journal of Geophysical Research: Solid Earth*, *111*(B5), B05407. https://doi.org/10.1029/2005JB003938

Breitfeld, H. T., Hennig-Breitfeld, J., BouDagher-Fadel, M., Schmidt, W. J., Meyer, K., Reinprecht, J., Lukie, T., Cuong, T. X., Hall, R., Kollert, N., Gough, A., & Ismail, R. (2022). Provenance of Oligocene–Miocene sedimentary rocks in the Cuu Long and Nam Con Son basins, Vietnam and early history of the Mekong River. *International Journal of Earth Sciences*, *111*(6), 1773–1804. https://doi.org/10.1007/s00531-022-02214-0

Brune, S., Heine, C., Clift, P. D., & Pérez-Gussinyé, M. (2017). Rifted margin architecture and crustal rheology: Reviewing Iberia-Newfoundland, central South Atlantic, and South China Sea. *Marine and Petroleum Geology*, *79*, 257–281. https://doi.org/10.1016/j.marpetgeo.2016.10.018

Buck, W. R. (1991). Modes of continental lithospheric extension. *Journal of Geophysical Research*, *96*, 20161–20178. https://doi.org/10.1029/91JB01485

Burton-Johnson, A., & Cullen, A. B. (2022). Continental rifting in the South China Sea through extension and high heat flow: An extended history. *Gondwana Research*, *120*, 235–263. https://doi.org/10.1016/j.gr.2022.07.015

Carter, A., Roques, D., & Bristow, C. S. (2000). Denudation history of onshore Central Vietnam: Constraints on the Cenozoic evolution of the western margin of the South China Sea. *Tectonophysics*, *322*, 265–277. https://doi.org/10.1016/S0040-1951(00)00091-3

Clark, M. K., & Royden, L. H. (2000). Topographic ooze: Building the eastern margin of Tibet by lower crustal flow. *Geology*, *28*, 703–706.

Clift, P., Lin, J., & Barckhausen, U. (2002). Evidence of low flexural rigidity and low viscosity lower continental crust during continental break-up in the South China Sea. *Marine and Petroleum Geology*, *19*(8), 951–970. https://doi.org/10.1016/S0264-8172(02)00108-3

Clift, P. D. (2006). Controls on the erosion of Cenozoic Asia and the flux of clastic sediment to the ocean. *Earth and Planetary Science Letters*, *241*(3–4), 571–580. https://doi.org/10.1016/j.epsl.2005.11.028

Clift, P. D., Brune, S., & Quinteros, J. (2015). Climate changes control offshore crustal structure at South China Sea continental margin. *Earth and Planetary Science Letters*, *420*, 66–72. https://doi.org/10.1016/j.epsl.2015.03.032

Clift, P. D., Carter, A., Campbell, I. H., Pringle, M., Hodges, K. V., Lap, N. V., & Allen, C. M. (2006). Thermochronology of mineral grains in the Song Hong and Mekong Rivers, Vietnam. *Geophysics, Geochemistry, Geosystems*, *7*(10), Q10005. https://doi.org/10.1029/2006GC001336

Clift, P. D., Hodges, K., Heslop, D., Hannigan, R., Hoang, L. V., & Calves, G. (2008). Greater Himalayan exhumation triggered by early Miocene monsoon intensification. *Nature Geoscience*, *1*, 875–880. https://doi.org/10.1038/ngeo351

Clift, P. D., Lee, G. H., Nguyen, A. D., Barckhausen, U., Hoang, V. L., & Sun, Z. (2008). Seismic evidence for a dangerous grounds mini-plate: No extrusion origin for the South China Sea. *Tectonics*, *27*, TC3008. https://doi.org/10.1029/2007TC002216

Clift, P. D., Lin, J., & ODP Leg 184 Scientific Party. (2001). Patterns of extension and magmatism along the continent-ocean boundary, South China margin. In R. C. L. Wilson, R. B. Whitmarsh, B. Taylor, & N. Froitzheim (Eds.), *Non-volcanic rifting of continental margins: A comparison of evidence from land and sea. Special Publication* (Vol. *187*, pp. 489–510). Geological Society London. https://doi.org/10.1144/GSL.SP.2001.187.01.2

Clift, P. D., Wan, S., & Blusztajn, J. (2014). Reconstructing chemical weathering, physical erosion and monsoon intensity since 25 ma in the northern South China Sea: A review of competing proxies. *Earth-Science Reviews*, *130*, 86–102. https://doi.org/10.1016/j.earscirev.2014.01.002

Cottam, M. A., Hall, R., & Ghani, A. A. (2013). Late cretaceous and Cenozoic tectonics of the Malay peninsula constrained by

thermochronology. *Journal of Asian Earth Sciences*, *76*, 241–257. https://doi.org/10.1016/j.jseaes.2013.04.029

Cottam, M. A., Hall, R., Sperber, C., Kohn, B. P., Forster, M. A., & Batt, G. E. (2013). Neogene rock uplift and erosion in northern Borneo: Evidence from the Kinabalu granite, mount Kinabalu. *Journal of the Geological Society*, *170*(5), 805–816. https://doi.org/10.1144/jgs2011-130

Cung, T. C., & Geissman, J. W. (2013). A review of the paleomagnetic data from cretaceous to lower tertiary rocks from Vietnam, Indochina and South China, and their implications for Cenozoic tectonism in Vietnam and adjacent areas. *Journal of Geodynamics*, *69*, 54–64. https://doi.org/10.1016/j.jog.2011.11.008

Davis, M., & Kusznir, N. J. (2004). Depth-dependent lithospheric stretching at rifted continental margins. In G. D. Karner (Ed.), *Proceedings of NSF rifted margins theoretical institute* (pp. 92–136). Columbia University Press. https://doi.org/10.7312/karn12738-005

Doglioni, C., Barba, S., Carminati, E., & Riguzzi, F. (2011). Role of the brittle–ductile transition on fault activation. *Physics of the Earth and Planetary Interiors*, *184*(3), 160–171. https://doi.org/10.1016/j.pepi.2010.11.005

Donelick, R. A., O'Sullivan, P. B., & Ketcham, R. A. (2005). Apatite fission-track analysis. *Reviews in Mineralogy and Geochemistry*, *58*(1), 49–94. https://doi.org/10.2138/rmg.2005.58.3

Dong, M., Zhang, J., Brune, S., Wu, S., Fang, G., & Yu, L. (2020). Quantifying Postrift lower crustal flow in the northern margin of the South China Sea. *Journal of Geophysical Research: Solid Earth*, *125*(2), e2019JB018910. https://doi.org/10.1029/2019JB018910

Driscoll, N. W., & Karner, G. D. (1998). Lower crustal extension across the northern Carnarvon basin, Australia: Evidence for an eastward dipping detachment. *Journal of Geophysical Research*, *103*, 4975–4991. https://doi.org/10.1029/97JB03295

Ehlers, T. A., & Farley, K. A. (2003). Apatite (U–Th)/He thermochronometry: Methods and applications to problems in tectonic and surface processes. *Earth and Planetary Science Letters*, *206*(1), 1–14. https://doi.org/10.1016/S0012-821X(02)01069-5

Franke, D., Barckhausen, U., Baristeas, N., Engels, M., Ladage, S., Lutz, R., Montano, J., Pellejera, N., Ramos, E. G., & Schnabel, M. (2011). The continent-ocean transition at the southeastern margin of the South China Sea. *Marine and Petroleum Geology*, *28*, 1187–1204. https://doi.org/10.1016/j.marpetgeo.2011.01.004

Franke, D., Barckhausen, U., Heyde, I., Tingay, M., & Ramli, N. (2008). Seismic images of a collision zone offshore NW Sabah/Borneo. *Marine and Petroleum Geology*, *25*(7), 606–624. https://doi.org/10.1016/j.marpetgeo.2007.11.004

Franke, D., Savva, D., Pubellier, M., Steuer, S., Mouly, B., Auxietre, J.-L., Meresse, F., & Chamot-Rooke, N. (2014). The final rifting evolution in the South China Sea. *Marine and Petroleum Geology*, *58B*, 704–720. https://doi.org/10.1016/j.marpetgeo.2013.11.020

Froitzheim, N., & Rubatto, D. (1998). Continental breakup by detachment faulting: Field evidence and geochronological constraints (Tasna nappe, Switzerland). *Terra Nova*, *10*(4), 171–176. https://doi.org/10.1046/j.1365-3121.1998.00187.x

Fyhn, M. B. W., Boldreel, L. O., & Nielsen, L. H. (2009). Geological development of the central and south Vietnamese margin: Implications for the establishment of the South China Sea, Indochinese escape tectonics and Cenozoic volcanism. *Tectonophysics*, *478*(3–4), 184–214. https://doi.org/10.1016/j.tecto.2009.08.002

Fyhn, M. B. W., Boldreel, L. O., & Nielsen, L. H. (2010). Escape tectonism in the Gulf of Thailand: Paleogene left-lateral pull-apart rifting in the Vietnamese part of the Malay Basin. *Tectonophysics*, *483*(3), 365–376. https://doi.org/10.1016/j.tecto.2009.11.004

Fyhn, M. B. W., Green, P. F., Bergman, S. C., Van Itterbeeck, J., Tri, T. V., Dien, P. T., Abatzis, I., Thomsen, T. B., Chea, S., Pedersen, S. A. S., Mai, L. C., Tuan, H. A., & Nielsen, L. H. (2016). Cenozoic deformation and exhumation of the Kampot Fold Belt and implications for South Indochina tectonics. *Journal of Geophysical Research: Solid Earth*, *121*(7), 5278–5307. https://doi.org/10.1002/2016JB012847

Gallagher, K., Brown, R., & Johnson, C. (1998). Fission track analysis and its applications to geological problems. *Annual Review of Earth and Planetary Sciences*, *26*(1), 519–572.

Gilley, L. D., Harrison, T. M., Leloup, P. H., Ryerson, F. J., Lovera, O. M., & Wang, J. H. (2003). Direct dating of left-lateral deformation along the Red River shear zone, China and Vietnam. *Journal of Geophysical Research*, *108*, 2127. https://doi.org/10.1029/2001JB001726

Gradstein, F. M., Ogg, J. G., Schmitz, M. D., & Ogg, G. M. (2020). *Geologic time scale 2020* (1358). Elsevier Science. ISBN: 9780128243619.

Hall, R. (1996). Reconstructing Cenozoic SE Asia. In R. Hall & D. J. Blundell (Eds.), *Tectonic evolution of Southeast Asia*. Special Publication (Vol. *106*, pp. 203–224). Geological Society. https://doi.org/10.1144/GSL.SP.1996.106.01.11

Hall, R. (2002). Cenozoic geological and plate tectonic evolution of SE Asia and the SW Pacific: Computer-based reconstructions and animations. *Journal of Asian Earth Sciences*, *20*, 353–434. https://doi.org/10.1016/S1367-9120(01)00069-4

Hall, R., & Morley, C. K. (2004). Sundaland basins. In P. Clift, P. Wang, W. Kuhnt, & D. E. Hayes (Eds.), *Continent-Ocean interactions within the east Asian marginal seas*. Geophysical Monograph (Vol. *149*, pp. 55–85). American Geophysical Union. https://doi.org/10.1029/149GM04

Hinz, K., Fritsch, J., Kempter, E. H. K., Mohammad, A. M., Meyer, J., Mohamed, D., Vosberg, H., Weber, J., & Benavidez, J. (1989). Thrust tectonics along the north-western continental margin of Sabah/Borneo. *Geologische Rundschau*, *78*(3), 705–730. https://doi.org/10.1007/BF01829317

Hinz, K., & Schlüter, H. U. (1985). Geology of the dangerous grounds, South China Sea, and the continental margin of Southwest Palawan: Results of Sonne cruises SO-23 and SO-27. *Energy*, *10*, 297–315.

Hoang, N., & Flower, M. (1998). Petrogenesis of Cenozoic basalts from Vietnam: Implication for origins of a 'diffuse Igneous Province'. *Journal of Petrology*, *39*(3), 369–395. https://doi.org/10.1093/petroj/39.3.369

Hoang, N., Flower, M. F. J., & Carlson, R. W. (1996). Major, trace element, and isotopic compositions of Vietnamese basalts: Interaction of hydrous EM1-rich asthenosphere with thinned Eurasian lithosphere. *Geochimica et Cosmochimica Acta*, *60*(22), 4329–4351. https://doi.org/10.1016/S0016-7037(96)00247-5

Hobbs, K. (2020). *Characterizing peridotite xenoliths from southern Vietnam: Insight into the underlying lithospheric mantle* [MS Thesis]. (89). University of Nebraska.

Hopper, J. R., & Buck, W. R. (1996). The effect of lower crustal flow on continental extension and passive margin formation. *Journal of Geophysical Research: Solid Earth*, *101*(B9), 20175–20194. https://doi.org/10.1029/96JB01644

Huang, H., Klingelhoefer, F., Qiu, X., Li, Y., & Wang, P. (2021). Seismic imaging of an Intracrustal deformation in the northwestern margin of the South China Sea: The role of a ductile layer in the crust. *Tectonics*, *40*(2), e2020TC006260. https://doi.org/10.1029/2020TC006260

Huchon, P., Nguyen, T. N. H., & Chamot-Rooke, N. (1998). Finite extension across the South Vietnam basins from 3D gravimetric modelling: Relation to South China Sea kinematics. *Marine and Petroleum Geology*, *15*, 619–634. https://doi.org/10.1016/S0264-8172(98)00031-2

Huchon, P., Nguyen, T. N. H., & Chamot-Rooke, N. (2001). Propagation of continental break-up in the south-western South China Sea. In R. C. L. Wilson, R. B. Whitmarsh, B. Taylor, & N. Froitzheim (Eds.), *Non-volcanic rifting of continental margins: A comparison of evidence from land and sea*. Special Publication (Vol. *187*, pp. 31–50). Geological Society. https://doi.org/10.1144/GSL.SP.2001.187.01.03

Huismans, R., & Beaumont, C. (2011). Depth-dependent extension, two-stage breakup and cratonic underplating at rifted margins. *Nature*, *473*, 74–79. https://doi.org/10.1038/nature09988

Hutchison, C. S. (2005). *Geology of north-West Borneo: Sarawak, Brunei and Sabah* (448). Elsevier. ISBN: 044455890X.

Hutchison, C. S. (2010). The north-West Borneo trough. *Marine Geology*, *271*, 32–43. https://doi.org/10.1016/j.margeo.2010.01.007

Hutchison, C. S., Bergman, S. C., Swauger, D. A., & Graves, J. E. (2000). A Miocene collisional belt in North Borneo: Uplift mechanism and isostatic adjustment quantified by thermochronology. *Journal of the Geological Society*, *157*, 783–793. https://doi.org/10.1144/jgs.157.4.783

Jagodziński, R., Sternal, B., Stattegger, K., & Szczuciński, W. (2020). Sediment distribution and provenance on the continental shelf off the Mekong River, SE Vietnam: Insights from heavy mineral analysis. *Journal of Asian Earth Sciences*, *196*, 104357. https://doi.org/10.1016/j.jseaes.2020.104357

Jahn, B. M., Zhou, X. H., & Li, J. L. (1990). Formation and tectonic evolution of southeastern China and Taiwan: Isotopic and geochemical constraints. *Tectonophysics*, *183*, 145–160. https://doi.org/10.1016/0040-1951(90)90413-3

Kassa, S., Tsegab, H., Sum, C. W., & CheeMeng, C. (2019). Fission-track data and U–Pb dating of granites from Cameron Highland, peninsular Malaysia: Evidence to comprehend exhumation episodes. *Data in Brief*, *25*, 104162. https://doi.org/10.1016/j.dib.2019.104162

Krähenbuhl, R. (1991). Magmatism, tin mineralization and tectonics of the Main range, Malaysian peninsula: Consequences for the plate tectonic model of Southeast Asia based on Rb-Sr, K-Ar and fission track data. *Geological Society of Malaysia Bulletin*, *29*, 1–100. https://doi.org/10.7186/bgsm29199101

Kusznir, N. J., Marsden, G., & Egan, S. S. (1991). A flexural cantilever simple shear/pure shear model of continental extension. In A. M. Roberts, G. Yielding, & B. Freeman (Eds.), *The geometry of Normal faults*. Special Publication (Vol. *56*, pp. 41–61). Geological Society. https://doi.org/10.1144/GSL.SP.1991.056.01.0

Lavier, L. L., & Manatschal, G. (2006). A mechanism to thin the continental lithosphere at magma-poor margins. *Nature*, *440*(7082), 324–328. https://doi.org/10.1038/nature04608

Lee, G. H., Lee, K., & Watkins, J. S. (2001). Geologic evolution of the Cuu Long and Nam Con Son basins, offshore southern Vietnam, South China Sea. *AAPG Bulletin*, *85*(6), 1055–1082. https://doi.org/10.1306/8626CA69-173B-11D7-8645000102C1865D

Lee, T. T., & Lawver, L. A. (1995). Cenozoic plate reconstruction of Southeast Asia. *Tectonophysics*, *251*, 85–138. https://doi.org/10.1016/0040-1951(95)00023-2

Lei, C., Alves, T. M., Ren, J., Pang, X., Yang, L., & Liu, J. (2019). Depositional architecture and structural evolution of a region immediately inboard of the locus of continental breakup (Liwan sub-basin, South China Sea). *GSA Bulletin*, *131*(7–8), 1059–1074. https://doi.org/10.1130/b35001.1

Li, C.-F., Li, J., Ding, W., Franke, D., Yao, Y., Shi, H., Pang, X., Cao, Y., Lin, J., Kulhanek, D. K., Williams, T., Bao, R., Briais, A., Brown, E. A., Chen, Y., Clift, P. D., Colwell, F. S., Dadd, K. A., Hernández-Almeida, I., … Zhao, X. (2015). Seismic stratigraphy of the central South China Sea basin and implications for neotectonics. *Journal of Geophysical Research*, *120*, 1377–1399. https://doi.org/10.1002/2014JB011686

Li, C.-F., Lin, J., Kulhanek, D. K., Williams, T., Bao, R., Briais, A., Brown, E. A., Chen, Y., Clift, P. D., Colwell, F. S., Dadd, K. A., Ding, W.-W., Hernández-Almeida, I., Huang, X.-L., Hyun, S., Jiang, T., Koppers, A. A. P., Li, Q., Liu, C., … Zhao, X. (2015). Site U1433. In *Proceedings of the International Ocean Discovery Program, 349: South China Sea Tectonics*. International Ocean Discovery Program. https://doi.org/10.14379/iodp.proc.349.105.2015

Li, C.-F., Xu, X., & Expedition 349 Scientific Party. (2014). Ages and magnetic structures of the South China Sea constrained by deep tow magnetic surveys and IODP expedition 349. *Geochemistry, Geophysics, Geosystems*, *15*, 4958–4983. https://doi.org/10.1002/2014GC005567

Li, J., Zhang, Y., Dong, S., & Johnston, S. T. (2014). Cretaceous tectonic evolution of South China: A preliminary synthesis. *Earth-Science Reviews*, *134*, 98–136. https://doi.org/10.1016/j.earscirev.2014.03.008

Li, L., Clift, P. D., & Nguyen, H. T. (2013). The sedimentary, magmatic and tectonic evolution of the southwestern South China Sea revealed by seismic stratigraphic analysis. *Marine Geophysical Research*, *34*, 393–406. https://doi.org/10.1007/s11001-013-9171-y

Li, L., Clift, P. D., Stephenson, R., & Nguyen, H. T. (2014). Non-uniform hyper-extension in advance of seafloor spreading on the Vietnam continental margin and the SW South China Sea. *Basin Research*, *26*, 106–134. https://doi.org/10.1111/bre.12045

Lin, A. T., & Watts, A. B. (2002). Origin of the West Taiwan basin by orogenic loading and flexure of a rifted continental margin. *Journal of Geophysical Research*, *107*(B9), 2185. https://doi.org/10.1029/2001JB000669

Lister, G. S., Etheridge, M. A., & Symonds, P. A. (1986). Detachment faulting and the evolution of passive continental margins. *Geology*, *14*, 246–250. https://doi.org/10.1130/0091-7613(1986)14<246:DFATEO>2.0.CO;2

Lister, G. S., Etheridge, M. A., & Symonds, P. A. (1991). Detachment models for the formation of passive continental margins. *Tectonics*, *10*, 1038–1064. https://doi.org/10.1029/90TC01007

Lithgow Bertelloni, C., & Gurnis, M. (1997). Cenozoic subsidence and uplift of continents from time-varying dynamic

topography. *Geology*, *25*, 735–738. https://doi.org/10.1130/0091-7613(1997)025<0735:CSAUOC>2.3.CO;2

Liu, C., Clift, P. D., Giosan, L., Miao, Y., Warny, S., & Wan, S. (2019). Paleoclimatic evolution of the SW and NE South China Sea and its relationship with spectral reflectance data over various age scales. *Palaeogeography, Palaeoclimatology, Palaeoecology*, *525*, 25–43. https://doi.org/10.1016/j.palaeo.2019.02.019

Liu, C., Clift, P. D., Murray, R. W., Blusztajn, J., Ireland, T., Wan, S., & Ding, W. (2017). Geochemical evidence for initiation of the modern Mekong Delta in the southwestern South China Sea after 8 ma. *Chemical Geology*, *451*, 38–54. https://doi.org/10.1016/j.chemgeo.2017.01.008

Lunt, P. (2019). A new view of integrating stratigraphic and tectonic analysis in South China Sea and North Borneo basins. *Journal of Asian Earth Sciences*, *177*, 220–239. https://doi.org/10.1016/j.jseaes.2019.03.009

Madon, M. B. (1997). Analysis of tectonic subsidence and heat flow in the Malay Basin (offshore peninsular Malaysia). *Bulletin of the Geological Society of Malaysia*, *41*, 95–108. https://doi.org/10.7186/bgsm41199709

Madon, M. B., & Watts, A. B. (1998). Gravity anomalies, subsidence history and the tectonic evolution of the Malay and Penyu basins (offshore peninsular Malaysia). *Basin Research*, *10*(4), 375–392. https://doi.org/10.1046/j.1365-2117.1998.00074.x

Maggi, A., Jackson, J. A., McKenzie, D., & Priestley, K. (2000). Earthquake focal depths, effective elastic thickness, and the strength of the continental lithosphere. *Geology*, *28*, 495–498. https://doi.org/10.1130/0091-7613(2000)28<495:EFDEET>2.0.CO;2

Matthews, S. J., Fraser, A. J., Lowe, S., Todd, S. P., & Peel, F. J. (1997). Structure, stratigraphy and petroleum geology of the SE Nam con Son Basin, offshore Vietnam. In A. J. Fraser, S. J. Matthews, & R. W. Murphy (Eds.), *Petroleum geology of Southeast Asia*. Special Publication (Vol. *126*, pp. 89–106). Geological Society. https://doi.org/10.1144/GSL.SP.1997.126.01.07

McKenzie, D., Nimmo, F., Jackson, J. A., Gans, P. B., & Miller, E. L. (2000). Characteristics and consequences of flow in the lower crust. *Journal of Geophysical Research: Solid Earth*, *105*(B5), 11029–11046. https://doi.org/10.1029/1999JB900446

McKenzie, D. P. (1978). Some remarks on the development of sedimentary basins. *Earth and Planetary Science Letters*, *40*, 25–32. https://doi.org/10.1016/0012-821X(78)90071-7

Miao, Y., Warny, S., Clift, P. D., Liu, C., & Gregory, M. (2017). Evidence of continuous Asian summer monsoon weakening as a response to global cooling over the last 8 ma. *Gondwana Research*, *52*(Supplement C), 48–58. https://doi.org/10.1016/j.gr.2017.09.003

Miller, K. G., Browning, J. V., Schmelz, W. J., Kopp, R. E., Mountain, G. S., & Wright, J. D. (2020). Cenozoic Sea-level and cryospheric evolution from deep-sea geochemical and continental margin records. *Science Advances*, *6*(20), eaaz1346. https://doi.org/10.1126/sciadv.aaz1346

Morley, C., & Searle, M. P. (2017). Regional tectonics, structure and evolution of the Andaman - Nicobar islands from ophiolite formation and obduction to collision and back-arc spreading. In P. C. Bandopadnyay & A. Carter (Eds.), *The Andaman-Nicobar accretionary ridge*. Memoir (Vol. *47*, pp. 51–74). Geological Society. https://doi.org/10.1144/M47

Morley, C. K. (2015). Five anomalous structural aspects of rift basins in Thailand and their impact on petroleum systems. In F. L. Richards, N. J. Richardson, S. J. Rippington, R. W. Wilson, & C. E. Bond (Eds.), *Industrial structural geology: Principles, techniques and integration*. Special Publications (Vol. *421*, pp. 143–168). Geological Society of London. https://doi.org/10.1144/SP421.2

Morley, C. K. (2016). Major unconformities/termination of extension events and associated surfaces in the South China seas: Review and implications for tectonic development. *Journal of Asian Earth Sciences*, *120*, 62–86. https://doi.org/10.1016/j.jseaes.2016.01.013

Morley, C. K., Promrak, W., Apuanram, W., Chaiyo, P., Chantraprasert, S., Ong, D., Suphawajruksakul, A., Thaemsiri, N., & Tingay, M. (2022). A major Miocene Deepwater mud canopy system: The North Sabah–Pagasa wedge, northwestern Borneo. *Geosphere*, *19*(1), 291–334. https://doi.org/10.1130/ges02518.1

Morley, C. K., & Racey, A. (2011). Tertiary stratigraphy. In M. F. Ridd, A. J. Barber, & M. J. Crow (Eds.), *The geology of Thailand* (pp. 223–270). Geological Society.

Morley, C. K., & Westaway, R. (2006). Subsidence in the superdeep Pattani and Malay basins of Southeast Asia: A coupled model incorporating lower- crustal flow in response to post-rift sediment loading. *Basin Research*, *18*, 51–84. https://doi.org/10.1111/j.1365-2117.2006.00285.x

Morley, R. J., & Morley, H. P. (2013). Mid Cenozoic freshwater wetlands of the Sunda region. *Journal of Limnology*, *72*(2), 18–35. https://doi.org/10.4081/jlimnol.2013.s2.e2

Morley, R. J., Swiecicki, T., & Pham, D. T. T. (2011). A sequence stratigraphic framework for the sunda region, based on integration of biostratigraphic, lithological and seismic data from Nam Con Son basin, Vietnam. 35th annual convention. Indonesian Petroleum Association, pp. IPA11-G-002.

Murray, M. R., & Dorobek, S. L. (2004). Sediment supply, tectonic subsidence, and basin-filling patterns across the southwestern South China Sea during Pliocene to recent time. In P. Clift, P. Wang, W. Kuhnt, & D. Hayes (Eds.), *Continent-ocean interactions within east Asian marginal seas*. Geophysical Monograph (Vol. *149*, pp. 235–254). American Geophysical Union. https://doi.org/10.1029/149GM13

Nachtergaele, S., Glorie, S., Morley, C., Charusiri, P., Kanjanapayont, P., Vermeesch, P., Carter, A., Ranst, G. V., & Grave, J. D. (2020). Cenozoic tectonic evolution of southeastern Thailand derived from low-temperature thermochronology. *Journal of the Geological Society*, *177*(2), 395–411. https://doi.org/10.1144/jgs2018-167

Nie, J., Ruetenik, G., Gallagher, K., Hoke, G., Garzione, C. N., Wang, W., Stockli, D., Hu, X., Wang, Z., Wang, Y., Stevens, T., Danišík, M., & Liu, S. (2018). Rapid incision of the Mekong River in the middle Miocene linked to monsoonal precipitation. *Nature Geoscience*, *11*(12), 944–948. https://doi.org/10.1038/s41561-018-0244-z

Nissen, S. S., Hayes, D. E., Buhl, P., Diebold, J., Yao, B., Zeng, W., & Chen, Y. (1995). Deep penetration seismic soundings across the northern margin of the South China Sea. *Journal of Geophysical Research*, *100*(B11), 22407–22433.

Peltzer, G., & Tapponnier, P. (1988). Formation and evolution of strike-slip faults, rifts, and basins during the India-Asia collision: An experimental approach. *Journal of Geophysical Research*, *93*, 15085–15117.

Pérez-Gussinyé, M., Morgan, J. P., Reston, T. J., & Ranero, C. R. (2006). The rift to drift transition at non-volcanic margins: Insights from numerical modelling. *Earth and Planetary*

Science Letters, *244*(1–2), 458–473. https://doi.org/10.1016/j.epsl.2006.01.059

Pubellier, M., & Morley, C. K. (2013). The basins of Sundaland (SE Asia): Evolution and boundary conditions. *Marine and Petroleum Geology*, *58*, 555–578. https://doi.org/10.1016/j.marpetgeo.2013.11.019

Reiners, P. W. (2005). Zircon (U-Th)/He Thermochronometry. *Reviews in Mineralogy & Geochemistry*, *58*, 151–179. https://doi.org/10.2138/rmg.2005.58.6

Replumaz, A., & Tapponnier, P. (2003). Reconstruction of the deformed collision zone between India and Asia by backward motion of lithospheric blocks. *Journal of Geophysical Research*, *108*(B6), 2285. https://doi.org/10.1029/2001JB000661

Reston, T. J., Krawczyk, C. M., & Klaeschen, D. (1996). The S-reflector west of Galicia (Spain): Evidence from prestack depth migration for detachment faulting during continental breakup. *Journal of Geophysical Research*, *101*(B4), 8075–8091. https://doi.org/10.1029/95JB03466

Roques, D., Rangin, C., & Huchon, P. (1997). Geometry and sense of motion along the Vietnam margin: Onshore/offshore Da Nang area. *Bulletin de la Société Géologique de France*, *168*, 413–422.

Royden, L., & Keen, C. E. (1980). Rifting processes and thermal evolution of the continental margin of eastern Canada determined from subsidence curves. *Earth and Planetary Science Letters*, *51*, 714–717. https://doi.org/10.1016/0012-821X(80)90216-2

Rutter, E. H. (1986). On the nomenclature of mode of failure transitions in rocks. *Tectonophysics*, *122*(3), 381–387. https://doi.org/10.1016/0040-1951(86)90153-8

Sarr, A. C., Husson, L., Sepulchre, P., Pastier, A. M., Pedoja, K., Elliot, M., Arias-Ruiz, C., Solihuddin, T., Aribowo, S., & Susilohadi. (2019). Subsiding Sundaland. *Geology*, *47*(2), 119–122. https://doi.org/10.1130/G45629.1

Sautter, B., Pubellier, M., Králiková Schlögl, S., Matenco, L., Andriessen, P., & Mathew, M. (2019). Exhumation of west Sundaland: A record of the path of India? *Earth-Science Reviews*, *198*, 102933. https://doi.org/10.1016/j.earscirev.2019.102933

Schmidt, W. J., Hoang, B. H., Handschy, J. W., Hai, V. T., Cuong, T. X., & Tung, N. T. (2019). Tectonic evolution and regional setting of the Cuu Long Basin, Vietnam. *Tectonophysics*, *757*, 36–57. https://doi.org/10.1016/j.tecto.2019.03.001

Scholz, C. H. (1998). Earthquakes and friction laws. *Nature*, *391*(6662), 37–42. https://doi.org/10.1038/34097

Sclater, J. G., & Christie, P. A. F. (1980). Continental stretching: An explanation of the post mid-cretaceous subsidence of the Central North Sea basin. *Journal of Geophysical Research*, *85*, 3711–3739. https://doi.org/10.1029/JB085iB07p03711

Sleep, N. H. (1990). Hotspots and mantle plumes: Some phenomenology. *Journal of Geophysical Research*, *95*, 6715–6736. https://doi.org/10.1029/JB095iB05p06715

Southeast Asian Research Group. (2022). *Heatflow. SE Asia Heatflow Database*. Royal Holloway, University of London. http://searg.rhul.ac.uk/current-research/heat-flow/

Su, D., White, N., & McKenzie, D. (1989). Extension and subsidence of the Pearl River mouth basin, northern South China Sea. *Basin Research*, *2*, 205–222. https://doi.org/10.1111/j.1365-2117.1989.tb00036.x

Sun, Z., Zhong, Z., Keep, M., Zhou, D., Cai, D., Li, X., Wu, S., & Jiang, J. (2009). 3D analogue modeling of the South China Sea: A discussion on breakup pattern. *Journal of Asian Earth Sciences*, *34*(4), 544–556. https://doi.org/10.1016/j.jseaes.2008.09.002

Tapponnier, P., Peltzer, G., Le Dain, A. Y., Armijo, R., & Cobbold, P. R. (1982). Propagating extrusion tectonics in Asia: New insights from simple experiments with plasticine. *Geology*, *10*, 611–616. https://doi.org/10.1130/0091-7613(1982)10<611:PETIAN>2.0.CO;2

Tjia, H. D., & Liew, K. K. (1996). Changes in tectonic stress field in northern Sunda shelf basins. In R. Hall & D. Blundell (Eds.), *Tectonic evolution of Southeast Asia*. Special Publications (Vol. *106*, pp. 291–306). Geological Society. https://doi.org/10.1144/GSL.SP.1996.106.01.19

Upton, D. R. (1999). *A regional fission track study of Thailand: Implications for thermal history and denudation* [Ph.D. Thesis]. (312). University of London.

Vail, P. R., Mitchum, R. M., Todd, R. G., Widmier, J. M., Thompson, S. I., Sangree, J. B., Bubb, J. N., & Hatlelid, W. G. (1977). Seismic stratigraphy and global changes of sea-level. In C. E. Payton (Ed.), *Seismic stratigraphy–applications to hydrocarbon exploration*. Memoir (Vol. *26*, pp. 49–212). American Association of Petroleum Geologists. https://doi.org/10.1306/M26490C3

Van Wagoner, J. C., Posamentier, H. W., Mitchum, R. M., Vail, P. R., Sarg, J. F., Loutit, T. S., Hardenbol, J., Wilgus, C. K., Hastings, B. S., Posamentier, H., Wagoner, J. V., Ross, C. A., & Kendall, C. G. S. C. (1988). An overview of the fundamentals of sequence stratigraphy and key definitions. In *Sea-level changes: An integrated approach* (Vol. *42*). SEPM Society for Sedimentary Geology. https://doi.org/10.2110/pec.88.01.0039

Vu, A. T., Fyhn, M. B. W., Xuan, C. T., Nguyen, T. T., Hoang, D. N., Pham, L. T., & Van, H. N. (2017). Cenozoic tectonic and stratigraphic development of the central Vietnamese continental margin. *Marine and Petroleum Geology*, *86*, 386–401. https://doi.org/10.1016/j.marpetgeo.2017.06.001

Walsh, J., Watterson, J., & Yielding, G. (1991). The importance of small-scale faulting in regional extension. *Nature*, *351*, 391–393. https://doi.org/10.1038/351391a0

Westaway, R. (1994). Re-evaluation of extension across the Pearl River Mouth Basin, South China Sea: Implications for continental lithosphere deformation mechanisms. *Journal of Structural Geology*, *16*, 823–838. https://doi.org/10.1016/0191-8141(94)90148-1

Westerhold, T., Marwan, N., Drury, A. J., Liebrand, D., Agnini, C., Anagnostou, E., Barnet, J. S. K., Bohaty, S. M., de Vleeschouwer, D., Florindo, F., Frederichs, T., Hodell, D. A., Holbourn, A. E., Kroon, D., Lauretano, V., Littler, K., Lourens, L. J., Lyle, M., Pälike, H., … Zachos, J. C. (2020). An astronomically dated record of Earth's climate and its predictability over the last 66 million years. *Science*, *369*(6509), 1383–1387. https://doi.org/10.1126/science.aba6853

Wheeler, P., & White, N. (2000). Quest for dynamic topography: Observations from Southeast Asia. *Geology*, *28*(11), 963–966. https://doi.org/10.1130/0091-7613(2000)28<963:QFDTOF>2.0.CO;2

White, R. S. (1999). The lithosphere under stress. *Philosophical Transactions of the Royal Society of London A: Mathematical, Physical and Engineering Sciences*, *357*(1753), 901–915. https://doi.org/10.1098/rsta.1999.0357

Wu, Y., Ding, W., Clift, P. D., Li, J., Yin, S., Fang, Y., & Ding, H. (2019). Sedimentary budget of the northwest sub-basin,

South China Sea: Controlling factors and geological implications. *International Geology Review*, *62*, 1–18. https://doi.org/10.1080/00206814.2019.1597392

Wu, Y., Ding, W., Sun, Z., Dong, C., & Fang, Y. (2018). Sedimentary budget of the southwest sub-basin, South China Sea: Controlling factors and geological implications. *Geological Journal*, *53*(6), 3082–3092. https://doi.org/10.1002/gj.3145

Xie, Z., Sun, L., Pang, X., Zheng, J., & Sun, Z. (2017). Origin of the Dongsha event in the South China Sea. *Marine Geophysical Research*, *38*(4), 357–371. https://doi.org/10.1007/s11001-017-9321-8

Zhang, X., Ye, X., Lv, J., Sun, J., & Wang, X. (2018). Crustal structure revealed by a deep seismic sounding profile of Baijing-Gaoming-Jinwan in the Pearl River Delta. *Journal of Ocean University of China*, *17*(1), 186–194. https://doi.org/10.1007/s11802-018-3489-7

How to cite this article: Clift, P. D., & Wilson, L. J. (2023). Syn- and post-rift lower crustal flow under the Sunda Shelf, southern Vietnam: A role for climatically modulated erosion. *Basin Research*, *00*, 1–30. https://doi.org/10.1111/bre.12809